

AD-A167 733

CHANNELIZATION CONSIDERATIONS FOR PSK MODULATION
TECHNIQUES IN FOLLOW-ON UHF MILSATCOM SYSTEMS(U)
M/A-COM LINKABIT INC VIENNA VA P CHAPPELL ET AL.

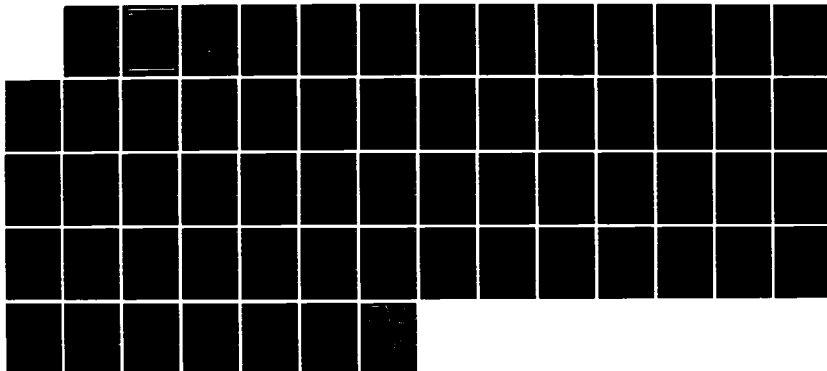
1/1

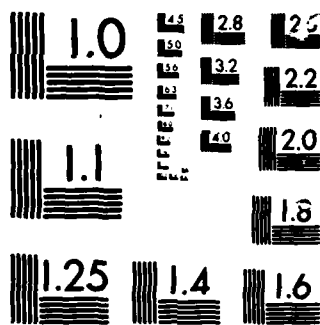
UNCLASSIFIED

30 APR 86 DCA100-84-C-0009

F/G 17/2.1

NL





MICROCOPY

CHART



GOVERNMENT SYSTEMS DIVISION

8619 WESTWOOD CENTER DRIVE
VIENNA, VA 22180

M/A-COM LINKABIT, Inc.
Log # MSO-86-037a
Copy # 22

AD-A167 733

**CHANNELIZATION CONSIDERATIONS FOR PSK
MODULATION TECHNIQUES IN FOLLOW-ON
UHF MILSATCOM SYSTEMS**

**FINAL REPORT
30 April 1986**

Submitted to
Defense Communications Agency
Center for Command and Control, and
Communications Systems, Code A800
8th & S. Courthouse Road
Arlington, VA 22204

Prepared by M/A-COM LINKABIT, Inc.
Under Contract DCA100-84-C-0009
Task MSO86-3, Subtask B

DTIC FILE COPY

DTIC
ELECTE
MAY 9 1986
A

This document has been approved
for public release and sale; its
distribution is unlimited.

CENTER FOR
COMMAND AND **C**ONTROL, AND
COMMUNICATIONS
SYSTEMS (C⁴S)

" EXCELLENCE IN C³ SYSTEMS FOR NATIONAL DEFENSE "

CHANNELIZATION CONSIDERATIONS FOR PSK
MODULATION TECHNIQUES IN FOLLOW-ON
UHF MILSATCOM SYSTEMS

April 1986



**DEFENSE
COMMUNICATIONS
AGENCY**

C⁴S _____
CY _____ OF _____ CYS

603208.0

TABLE OF CONTENTS

EXECUTIVE SUMMARY	ES-1
CHAPTER 1 - INTRODUCTION	1-1
1.1 Objective	1-1
1.2 Background	1-1
CHAPTER 2 - TASK DESCRIPTION	2-1
2.1 Study Scope	2-1
2.2 Study Methodology	2-3
2.3 Description of Simulator	2-4
2.3.1 Overview	2-4
2.3.2 PSK Demodulators	2-5
2.3.3 ACI Model	2-9
2.3.4 BER Estimator	2-9
CHAPTER 3 - SIMULATOR VERIFICATION	3-1
3.1 Demodulator Performance	3-1
3.2 Channel and ACI Spectra	3-1
3.3 Simulator Performance Verification	3-3
CHAPTER 4 - RESULTS	4-1
4.1 Required E_b/N_0 for Given P_e vs. Filter BT	4-1
4.1.1 BPSK - 5-kHz Channels	4-1
4.1.2 SBPSK - 5-kHz Channels	4-3
4.1.3 QPSK - 25-kHz Channels	4-3
4.1.4 OQPSK - 25-kHz Channels	4-6
4.2 Required E_b/N_0 for Given P_e vs. BT with Increased Power Interferers	4-6
4.2.1 BPSK - 5-kHz Channels	4-8
4.2.2 SBPSK - 5-kHz Channels	4-11
4.2.3 BPSK - 25-kHz Channels	4-11
4.2.4 SBPSK - 25-kHz Channels	4-15
CHAPTER 5 - SUMMARY AND CONCLUSIONS	5-1
5.1 Summary	5-1
5.2 Conclusions	5-4
5.3 Recommendations for Future Study	5-7
APPENDIX A - REFERENCES	A-1
APPENDIX B - COMPARISON TO PREVIOUS RESULTS	B-1

LIST OF FIGURES

2-1	Block Diagram of Channel Model Used in Present Study	2-4
2-2	Detector for BPSK Signal. Polarity of Samples Determines the Bit Present During the kth Symbol Period	2-5
2-3	SBPSK Probability of Error with Integrate and Dump Detector	2-7
2-4	Detector for QPSK Signal	2-8
2-5	Simulator Channel Model Including ACI	2-10
3-1	BPSK Spectrum at Input to Channel Filter. Equal Power Interferers at $\pm 4.167 \times R_s$	3-2
3-2	BPSK Spectrum at Input to Demodulator. Channel Characteristics: Equal Power Interferers at $4.167 \times R_s$; 8-Pole Butterworth	3-2
3-3	Verification of Simulator BER Estimates Theory of PSK with Gaussian Noise Interference	3-4
4-1	Performance of BPSK for Selected 8-Pole Filters. Channel Characteristics: $R_s = I/T = 2400$ sps; Equal Power Interferers at ± 10 kHz; Balanced Uplink and Downlink Noise Levels; 5-kHz Channels	4-2
4-2	Performance of SBPSK for Selected 8-Pole Filters. Channel Characteristics: $R_s = I/T = 2400$ sps; Equal Power Interferers at ± 10 kHz; Balanced Uplink and Downlink Noise Levels; 5-kHz Channels	4-4
4-3	Performance of QPSK for Selected 8-Pole Filters. Channel Characteristics: $R_s = I/T = 16000$ sps; Equal Power Interferers at ± 50 kHz; Balanced Uplink and Downlink Noise Levels; 25-kHz Channels	4-5
4-4	Performance of OQPSK for Selected 8-Pole Filters. Channel Characteristics: $R_s = I/T = 16000$ sps; Equal Power Interferers at ± 50 kHz; Balanced Uplink and Downlink Noise Levels; 25-kHz Channels	4-7
4-5	Performance of BPSK for Selected 8-Pole Filters. Channel Characteristics: $R_s = I/T = 1200$ sps; ± 3 -dB Power Interferers at ± 5 kHz; Balanced Uplink and Downlink Noise Levels; 5-kHz Channels	4-9
4-6	Performance of BPSK for Selected 8-Pole Filters. Channel Characteristics: $R_s = I/T = 1200$ sps; ± 10 -dB Power Interferers at ± 10 kHz; Balanced Uplink and Downlink Noise Levels; 5-kHz Channels	4-10
4-7	Performance of SBPSK for Selected 8-Pole Filters. Channel Characteristics: $R_s = I/T = 2400$ sps; ± 3 -dB Power Interferers at ± 5 kHz; Balanced Uplink and Downlink Noise Levels; 5-kHz Channels	4-12
4-8	Performance of SBPSK for Selected 8-Pole Filters. Channel Characteristics: $R_s = I/T = 2400$ sps; ± 10 -dB Power Interferers at ± 10 kHz; Balanced Uplink and Downlink Noise Levels; 5-kHz Channels	4-13

LIST OF FIGURES (Cont'd)

- 4-9 Performance of BPSK for Selected 8-Pole Filters.
 Channel Characteristics: $R_s = I/T = 19.2$ ksps;
 +10-dB Power Interferers at ± 50 kHz; Balanced
 Uplink and Downlink Noise Levels; 25-kHz Channels 4-14
- 4-10 Performance of BPSK for Selected 8-Pole Filters.
 Channel Characteristics: $R_s = I/T = 19.2$ ksps;
 +10-dB Power Interferers at ± 100 kHz; Balanced
 Uplink and Downlink Noise Levels; 25-kHz Channels 4-16
- 4-11 Performance of SBPSK for Selected 8-Pole Filters.
 Channel Characteristics: $R_s = I/T = 19.2$ ksps;
 +10-dB Power Interferers at ± 50 kHz; Balanced
 Uplink and Downlink Noise Levels; 25-kHz Channels 4-17
- 4-12 Performance of SBPSK for Selected 8-Pole Filters.
 Channel Characteristics: $R_s = I/T = 19.2$ ksps;
 +10-dB Power Interferers at ± 100 kHz; Balanced
 Uplink and Downlink Noise Levels; 25-kHz Channels 4-18



Per Form 50	
By	
Date	
Time	
Special	
A1	1

LIST OF TABLES

ES-1	Summary of Filter Performance of 5-kHz Channels at 1×10^{-3} Channel Error Rate	ES-2
ES-2	Summary of Filter Performance of 25-kHz Channels at 5×10^{-2} Channel Error Rate	ES-3
3-1	Ninety Percent Confidence Intervals for n Errors and Probability of Error, p	3-5
5-1	Summary of Filter Performance of 5-kHz Channels at 1×10^{-3} Channel Error Rate	5-5
5-2	Summary of Filter Performance of 25-kHz Channels at 5×10^{-2} Channel Error Rate	5-6
B-1	Comparison of Modulation Simulation Model with Additive Noise Approximate Model	B-2
B-2	Comparison of Degradation of Additive Noise Approximation to Modulation Simulation	B-4

EXECUTIVE SUMMARY

The purpose of this report is to develop tradeoffs and requirements on channel spacing for the follow-on FLTSAT/LEASAT UHF MILSATCOM satellite system given realistic operating conditions where high-power and low-power terminals may be located on adjacent channel frequencies. Results obtained here can be used to develop guidelines on expected system performance and/or specifications on allowable losses due to adjacent channel interference and inband channel filtering losses.

This report presents the results of MILSATCOM UHF 5-kHz and 25-kHz nonlinear (hardlimited) channel performance as a function of modulation type and symbol rate, filter characteristics (type), and adjacent channel spacing. The primary channel performance measure is transmitted bit energy per channel noise (E_b/N_0) versus probability of bit error. Filter bandwidth is expressed as a BT product, where B is the two-sided 3-dB bandwidth and T is the symbol rate.

Table ES-1 lists the results of the simulation effort for 5-kHz channels in terms of filter types and the performance for the configurations investigated. Channel spacings of 5 kHz and 10 kHz were chosen for simulation because these values are compatible with existing equipment. Future systems, in order to maintain this compatibility, will specify the same or similar values for channel spacing. A $P_e = 1 \times 10^{-3}$ bit error rate was chosen as a benchmark because this is approximately the maximum acceptable error rate for uncoded voice transmission. For the channel configurations studied, the following observations may be made:

- Regardless of filter type and channel spacing, filter designs with BT products in the range 1.6 to 2.2 provide comparable performance.

- For 50-percent shaped binary phase shift keying (SBPSK), adjacent channel interference (ACI) has minimal impact on system performance for channel spacings of 10 kHz.
- Bessel filters, because of their low phase distortion, provide the flattest performance over the range of filter BT products studied.
- SBPSK, because of its spectral efficiency, provides better system performance under stringent channel configurations of narrow spacing and high adjacent channel power.

Table ES-1. Summary of Filter Performance for 5 kHz Channels at 1×10^{-3} Channel Error Rate

MODULATION TYPE	SYMBOL RATE	ADJACENT CHANNEL SPACING	ACI POWER ($S_u / S_d = S_u / S_d$)	FILTER TYPE *	E_b / N_0 AT OPTIMUM BT PRODUCT†
BPSK	2400 (bps)	10 (kHz)	0 (dB)	B	7.0 (dB)
				C	7.3
				S	6.8
BPSK	1200	5	3	B,S	6.9
				C	7.2
BSPK	1200	10	10	B,C,S	7.0
SBPSK	2400	10	0	B,S	7.2
				C	7.3
SBPSK	2400	5	3	B	9.3
				C	10.2
				S	9.7
SBPSK	2400	10	10	B	7.4
				C	7.7
				S	7.6

* B = BUTTERWORTH, C = CHEBYSHEV, S = BESSEL

† REQUIRED THEORETICAL $E_b/N_0 = 6.8$ dB

604230.0

Table ES-2 presents the results of 25-kHz channel configurations. Channel spacings of 50 kHz and 100 kHz were chosen for simulation because these values are compatible with existing equipment. Future systems, in order to maintain this compatibility, will specify the same or similar values for channel spacing. A $P_e = 5 \times 10^{-2}$ error rate was chosen as a benchmark because this is the channel error rate corresponding to a decoded error rate of $P_e = 1 \times 10^{-5}$ for $K=7$, $R=1/2$, convolutional coding with soft-decision (3-bit) decoding. Therefore, although the values are given in terms of E_b/N_0 , it is the channel symbol energy that is measured. Similar trends noted for the 5-kHz channels are apparent. Specifically:

- Filter BT products in the range 1.6 to 2.2 provide comparable performance regardless of filter type and channel spacing.
- ACI has minimal impact on system performance for channel spacings of 100 kHz.
- Bessel filters provide the best system performance over the range of filter BTs studied.
- The spectral efficiency of SBPSK improves system performance only under conditions of close channel spacing (50 kHz) and high adjacent channel interfering power.

→ In general, for most simulated configurations, the system is insensitive to filter type and ACI. ACI has an impact only under conditions of narrow channel spacing (e.g., 5 kHz for 5-kHz channels and 50 kHz for 25-kHz channels) and high adjacent channel interference power. Under these conditions, SBPSK and OQPSK provided better E_b/N_0 performance than BPSK and QPSK. Performance sensitivity due to filter type were found to be, at most, approximately 0.5 dB.

Table ES-2. Summary of Filter Performance for 25 kHz Channels at 5×10^{-2} Channel Error Rate

MODULATION TYPE	SYMBOL RATE	ADJACENT CHANNEL SPACING	ACI POWER ($S_u / S_d = S_i / S_d$)	FILTER TYPE*	E_b / N_0 AT OPTIMUM BT PRODUCT†
BPSK	19200 (bps)	50 (kHz)	10 (dB)	B,S C	3.9 (dB) 4.2
BPSK	19200	100	10	B,S C	2.2 2.5
SBPSK	19200	50	10	B,S C	2.6 2.8
SBPSK	19200	100	10	B,S C	1.9 2.0
QPSK	16000	50	0	B,S C	2.1 2.4
OQPSK	16000	50	0	B C S	1.5 1.6 1.7

* B = BUTTERWORTH, C = CHEBYSHEV, S = BESSEL

† REQUIRED THEORETICAL $E_b / N_0 = 1.3$ dB
WITH 3-BIT SOFT-DECISION VITERBI CODING

604232.0

CHAPTER 1

INTRODUCTION

1.1 OBJECTIVE

The purpose of this task is to study the effects of system parameter variations on the bit error rate (BER) performance of various PSK modulation techniques in a bandlimited nonlinear UHF MILSATCOM channel. This report presents the methodology used in the study as well as the results that have been obtained for selected channel configurations.

1.2 BACKGROUND

This task is a follow-on to a previous study [Ref. 1] that investigated the fractional out-of-band power characteristics of several PSK modulation techniques in a nonlinear UHF MILSATCOM channel. The previous study's scope was limited to the determination of ACI that would fall inband as a function of selected channel parameters. It was concluded that although ACI power levels were of great interest, the ultimate goal was the optimization of energy per bit-to-noise power density ratio, E_b/N_0 , versus bit error rate. Chapter 2 presents a discussion of the differences between the current and previous studies.

A goal of communications systems development is to design a system that achieves a BER performance with minimum power and bandwidth requirements at a reasonable cost and complexity. This goal can be achieved by an analysis of tradeoffs of selected system parameters, including channel filters, PSK modulator type, and ACI levels.

The principal design parameter to be investigated is the choice of filter that minimized both intersymbol interference (ISI) and ACI for a given channel spacing and transmission rate. In general, ISI and ACI effects are complementary; that is, reducing one effect will increase the other.

The following chapter describes the communications channel model parameters and the methodology employed to quantify the effects of parameter variations on system performance.

CHAPTER 2

TASK DESCRIPTION

2.1 STUDY SCOPE

This study is concerned primarily with the follow-on FLTSAT/LEASAT MILSATCOM UHF communications channel. The parameters chosen for investigation are those expected to be typical for this system. The general parameter categories of interest in this task are channel bandwidth, modulation type, symbol rate, channel filter type, and channel spacing. The ultimate measure of a particular combination of these parameters is the BER performance versus the required energy per bit-to-noise power density ratio, E_b/N_0 , of the channel resulting from the combination of these component parameters.

For the MILSATCOM UHF system of interest, the two channel bandwidths are 5 kHz and 25 kHz.

The modulation category consists of the following PSK types:

- Binary PSK (BPSK)
- Quaternary PSK (QPSK)
- 50% Shaped BPSK (SBPSK)
- Offset QPSK (OQPSK).

These modulation types and simulation details have been described in detail in Ref. 1.

The channel filter families chosen for study provide a diverse range of filter effects that permit a comparative analysis of their performance. The filters are all pole (no special inband equalization), which provides a worst-case bound on performance for the UHF satellite system under consideration.

Following is a list of these filters along with a summary highlighting their key properties:

- Bessel
 - Low passband group delay distortion (i.e., highly linear inband phase response)
 - Relatively slow out-of-band magnitude rolloff
- Chebyshev
 - Relatively large passband group delay and phase distortion
 - Rapid transition/stopband magnitude rolloff
- Butterworth
 - Moderate passband phase distortion (less than Chebyshev, more than Bessel)
 - Relatively flat passband magnitude response.

The channel filter bandwidths discussed in this report are all normalized to symbol rate and are therefore expressed as a BT-product (bandwidth x symbol period). The convention followed throughout this report is to employ the filter's double-sided 3-dB bandwidth (i.e., the RF 3-dB bandwidth) in BT-product calculation.

For this analysis, filter BT products between approximately 1.0 to 4.0 were selected to cover the full range of practical filter designs. Filters with BT products less than 1.0 produce excessively high ISI; filters with BT products greater than 4.0 result in unacceptably high ACI for the channel spacings of interest.

The transmission symbol rate and channel spacing categories are dependent on the nominal channel bandwidth. For the 5-kHz and 25-kHz MILSATCOM UHF channels of interest, the following channel spacings and symbol rates have been chosen:

- 5-kHz Channels:

- 1.2 ksps (BPSK), 5-kHz and 10-kHz spacing
- 2.4 ksps (BPSK, SBPSK), 5-kHz and 10-kHz spacing

- 25-kHz Channels:

- 16 ksps (QPSK, OQPSK), 50-kHz and 100-kHz spacing
- 19.2 ksps (BPSK, SBPSK) 50-kHz and 100-kHz spacing.

2.2 STUDY METHODOLOGY

The scope of the study outlined in the previous section requires that numerous channel parameters must be varied to gain an understanding of their interactions in combination. Direct analytic study of each parameter variation is complicated by the presence of a nonlinear element (a hardlimiter) used in MILSATCOM UHF satellites to permit a common amplifier for a multi-channel system. The most flexible and rapid approach in obtaining results for this system is through the use of a computer simulation.

The previous study [Ref. 1] developed a simulator as a tool to estimate the fractional out-of-band power of several PSK modulation techniques used in a nonlinear UHF channel. Results obtained in the present study build on the previous work and extend the simulator's capability to model the complete channel and estimate its performance in terms of bit error probability versus E_b/N_0 .

A block diagram of the current simulation is shown in Figure 2-1. The simulator employs a conventional Monte Carlo technique to obtain an estimate of system performance (bit error probability) as a function of channel configuration and additive white Gaussian noise. An indepth discussion of each simulator component is given in the next chapter.

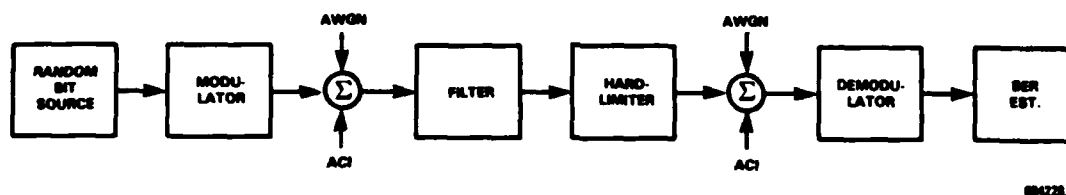


Figure 2-1. Block Diagram of Channel Model Used in Present Study

2.3 DESCRIPTION OF SIMULATOR

2.3.1 Overview

The channel simulator, shown in Figure 2-1, has been designed to provide a flexible baseband model of a typical bandlimited nonlinear satellite channel with random input data. Modulation types supported by the simulator are BPSK, SBPSK, QPSK, and OQPSK. The characteristics of the PSK modulators are described in detail in Ref. 1.

Available filter types are Bessel, Butterworth, and Chebyshev. In each case the filter is realized by computing samples of the filter transfer function. Signal filtering is accomplished in the frequency domain and then inverse-transformed to obtain the output sequence in the time domain. A detailed description of the filter characteristics and the filtering algorithm are found in Ref. 1.

The channel nonlinearity is modeled by an ideal hardlimiter whose transfer characteristic is described by

$$V_o(t) = V_i(t) / |V_i(t)| \quad (2.1)$$

where $V_i(t)$ and $V_o(t)$ are the input and output voltages, respectively. The magnitude of the input is normalized while the phase angle is preserved.

The following sections describe the additions to the simulator that were made for this study.

2.3.2 PSK Demodulators

2.3.2.1 BPSK Demodulator

The BPSK signal, defined over one symbol period (T_s) as

$$s(t) = \cos(\omega_c t + \theta_k) ; \theta_k = 0, \pi, \quad (2.2)$$

$$kT_s \leq t \leq (k+1)T_s$$

is demodulated with the matched-filter receiver shown in Figure 2-2. This is the optimum detector for the undistorted BPSK signal in the presence of white noise [Ref. 2]. Since the waveform is modeled as a discrete signal in the simulator, the integration is performed by a summation of the signal samples over a single symbol period.

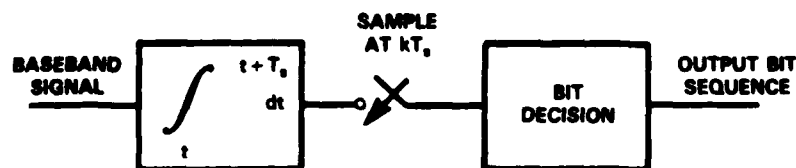


Figure 2-2. Detector for BPSK Signal. Polarity of Samples Determines the Bit Present During the k th Symbol Period

The threshold level for bit decisions is zero volts, since the input sequence is random with equally likely symbols. Accurate symbol timing is derived from the input sequence by measuring the channel group delay with a modulated preamble signal in a noise-free channel.

2.3.2.2 SBPSK Demodulator

The SBPSK signal is defined as

$$s(t) = \cos(\omega_c t + \theta(t)) ; kT_s \leq t \leq (k+1)T_s \quad (2.3)$$

where the phase function $\theta(t)$ provides a constant rate phase rotation determined by the shaping factor during data transitions and a constant phase during the remainder of the symbol period [Refs. 1,5].

In order to provide the closest possible approximation to MILSATCOM operational implementation, the SBPSK signal in the simulator is demodulated with the same receiver designed for the BPSK signal. Because of this implementation, the receiver performance is degraded by a loss in detector efficiency through the use of this simpler, lower cost BPSK detector.

The loss in detection efficiency incurred through the use of the BPSK detector is a function of the degree of shaping, as shown in Figure 2-3. This loss is simply a measure of the signal power in the quadrature-phase (Q) channel that results from the shaping operation, since the information in the Q-channel is not used in the detection process. For 50-percent shaping the loss is approximately 1.25 dB.

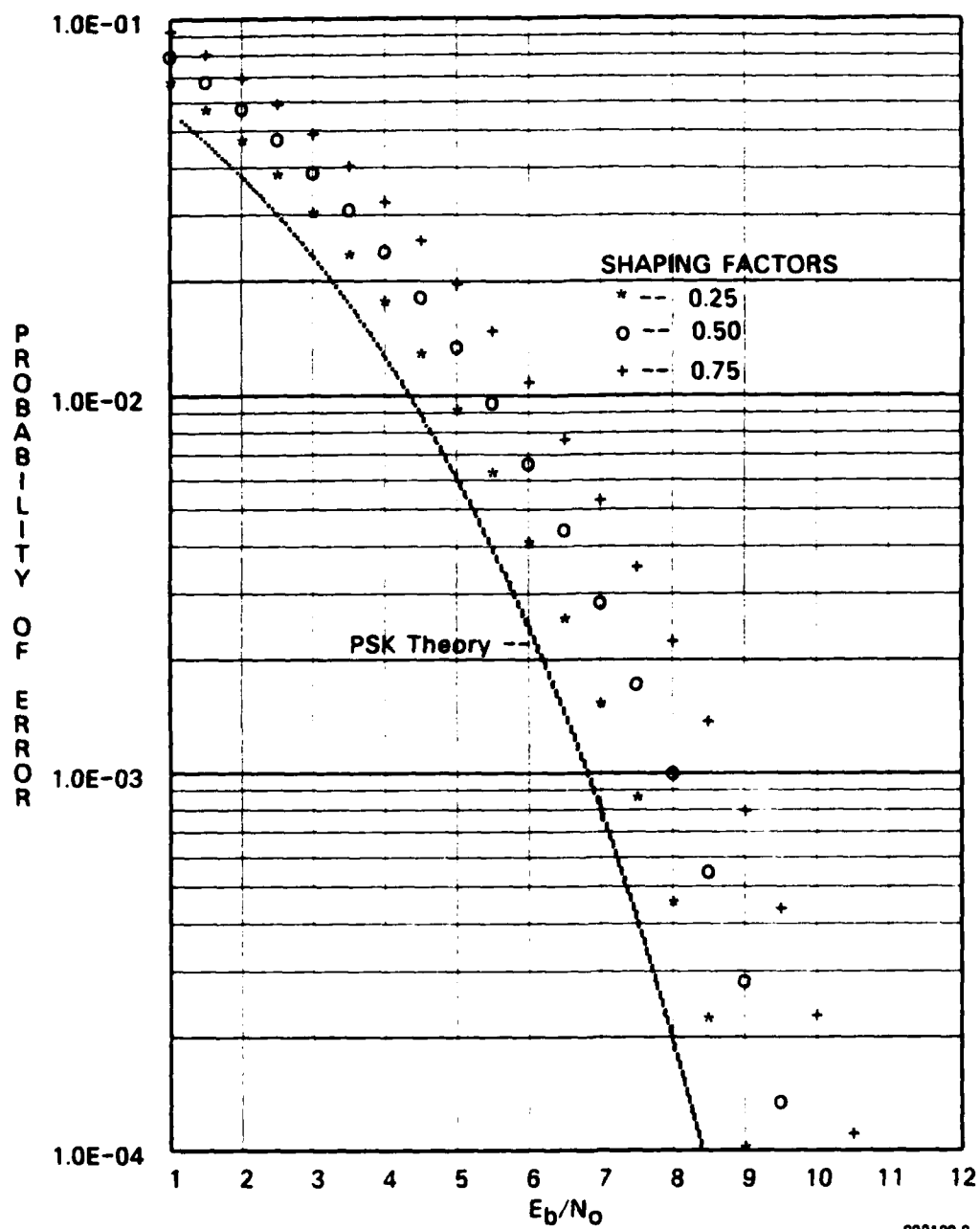


Figure 2-3. SBPSK Probability of Error with Integrate and Dump Detector.
Note that all Quadrature Channel Information is Neglected
as in Existing Low-Cost Equipment Designs

2.3.2.3 QPSK Demodulator

The QPSK signal is defined as:

$$s(t) = \cos(\omega_c t + \theta_k) ; \theta_k = 0, \pi/2, \pi, 3\pi/2, \quad (2.4)$$

$$kT_s \leq t \leq (k+1)T_s$$

QPSK demodulation is similar to BPSK demodulation. The QPSK demodulator consists of two separate (I and Q channel) BPSK detectors in parallel as shown in Figure 2-4. Since the waveform is represented at baseband in the simulator, the I and Q channel signals are available without the need for downconverting from a carrier frequency. The I and Q channel output bit streams are multiplexed into the final output bit sequence.

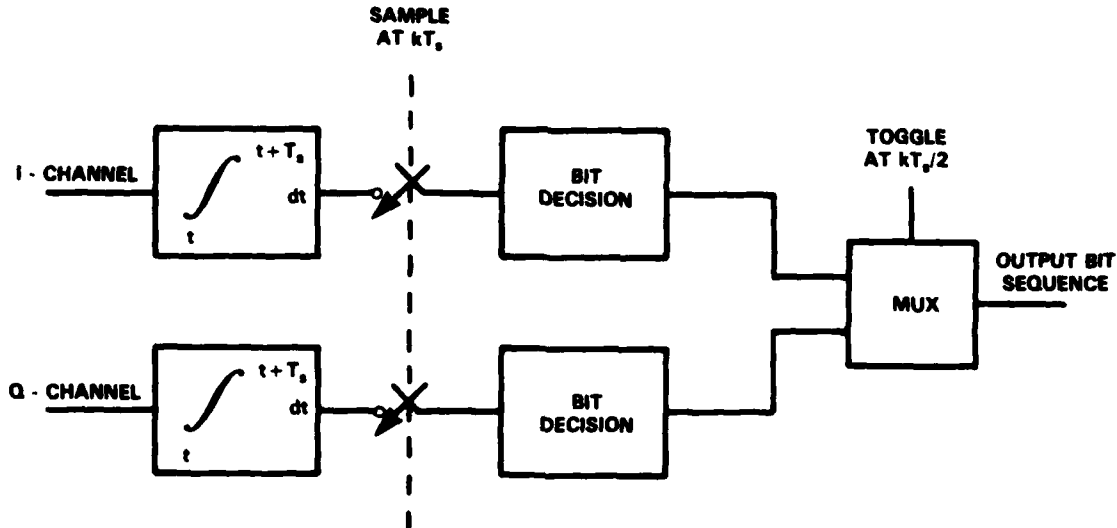


Figure 2-4. Detector for QPSK Signal

2.3.2.4 OQPSK Demodulator

The OQPSK signal is also described by Equation (2.4). However, the data transitions in the I and Q channels are staggered by half the symbol period, $T_s/2$. The OQPSK demodulator uses the same basic configuration as the QPSK demodulator. The difference is that a delay of the $T_s/2$ is introduced in the Q-channel before the integrate-and-dump filter. The delay accounts for the time offset between the I and Q channel bit transitions.

2.3.3 ACI Model

The channel block diagram, including the ACI model, is shown in Figure 2-5. Each adjacent channel bit sequence is a delayed, frequency-offset version of the central channel bit sequence. The delays, $T_n(t)$, are composed of a large fixed delay that ensures statistical independence between ACI and desired signals and a small time varying delay that simulates clock drift. The frequency offset of the ACI signals is indicated by the multiplicative factor $\exp(\pm j \omega_o t)$ where $\pm \omega_o$ is the radian frequency offset above/below the desired channel center frequency.

Note that the downlink adjacent channel interferers are assumed to be from a source identical to the central channel, which has interference on both sides. This means that, in effect, the simulation includes ACI from more than two adjacent channels. However, the effect of these non-adjacent channels will be very small because they are almost totally rejected by the channel filter.

2.3.4 BER Estimator

Several techniques exist for estimating the bit error rate in the simulation of a digital communications system [Ref. 3].

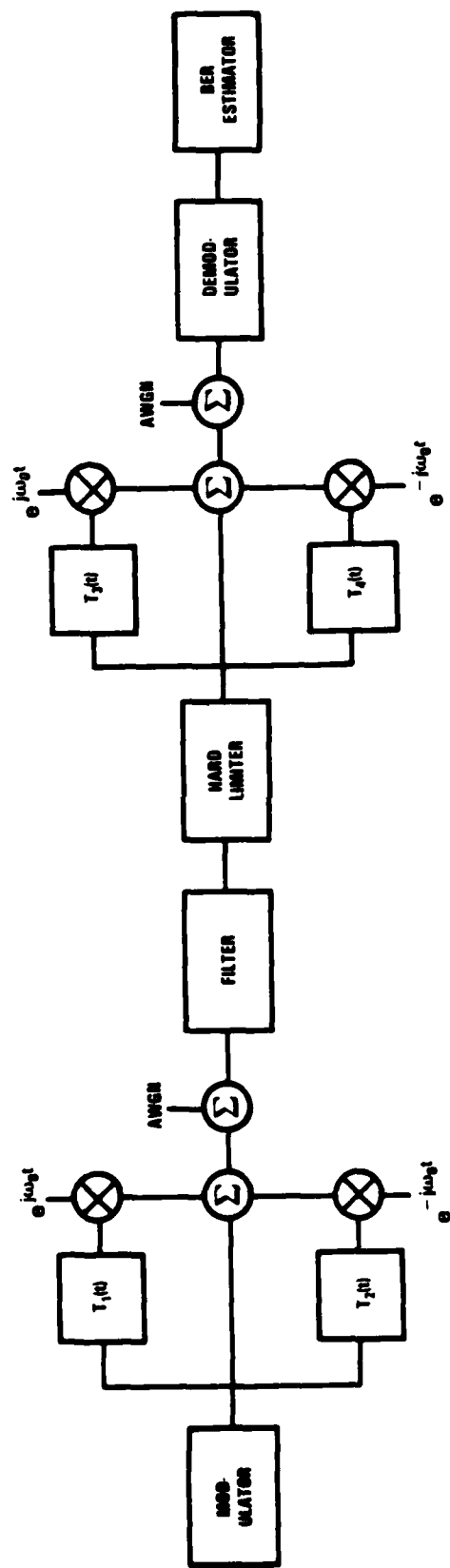


Figure 2-5. Simulator Channel Model Including ACI

603145.0

For this simulator the Monte Carlo or error counting method is used because it is not dependent on the properties of the interferers and is relatively simple to implement.

With this method the bit error rate is estimated by directly counting the errors generated by a comparison of the known input sequence to the output sequence determined by the model. The BER estimate is then given by n/N , where n is the number of bits in error and N is the total number of bits.

CHAPTER 3

SIMULATOR VERIFICATION

3.1 DEMODULATOR PERFORMANCE

Two of the critical parameters that were verified for each demodulator design are the received symbol timing and phase. These were verified by observing the integrate-and-dump outputs for a modulated bit sequence in the noiseless channel. Symbol timing and phase were verified for a number of filters to ensure that the effects of group delay and phase rotation caused by the filters did not degrade performance. After compensation for group delay, symbol timing was accurate within the sampling accuracy. A phase rotation error of less than 6 degrees was observed for all filters under consideration. Because these minor phase offsets had negligible impact on simulator performance, corrections for their effects were unnecessary.

3.2 CHANNEL AND ACI SPECTRA

The central channel and ACI time domain signals were observed to be consistent with the symbol timing and clock drift functions in the ACI module. To verify the modulation operation, it is useful to observe the signal spectrum with ACI. For example, Figure 3-1 shows the BPSK spectrum with ACI at $4.1666 \times R_s$ (e.g., 10-kHz spacing for 2.4 kbps), where R_s is the symbol rate. Figure 3-2 shows the signal in the same channel configuration as in Figure 3-1 subsequent to filtering and hardlimiting. In these cases, a check of the symmetry and rolloff of the spectra indicates that the ACI modules are operating properly.

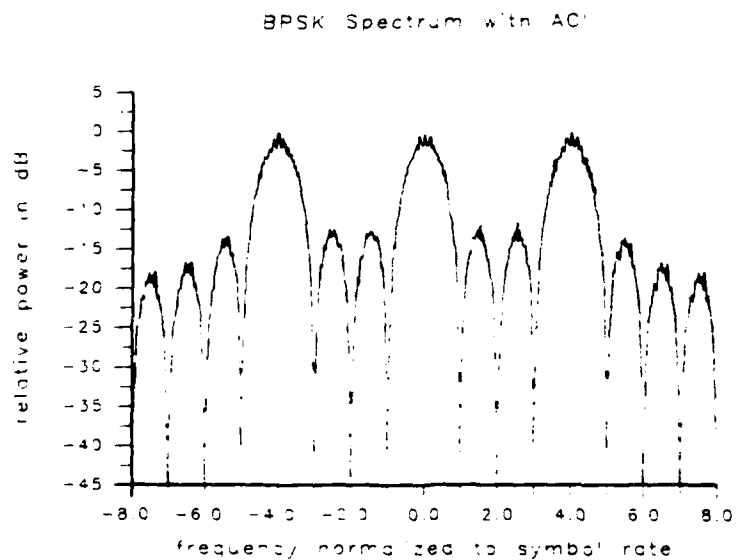


Figure 3-1. BPSK Spectrum at Input to Channel Filter. Equal Power Interferers at $\pm 4.167 \times R_s$

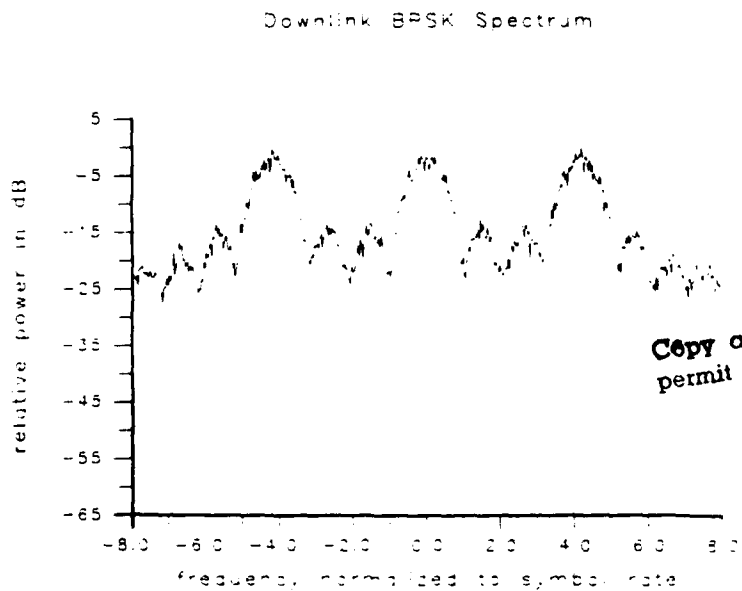


Figure 3-2. BPSK Spectrum at Input to Demodulator. Channel Characteristics: Equal Power Interferers at $4.167 \times R_s$; 8-Pole Butterworth

603187.0

3.3 SIMULATOR PERFORMANCE VERIFICATION

Overall simulator performance was verified by comparing measured BER results using gaussian noise interference to the known theoretical BER.

Figure 3-3 presents these results for all the modulation types. A total of 20,090 bits were used for each simulation data point shown in Figure 3-3. The results are in close agreement with theory. As discussed in Section 2.3.2.2, there is an inherent 1.25-dB loss for SBPSK with 50-percent shaping due to the use of a simple, low-cost receiver design. Thus, the SBPSK simulation results are exactly as predicted, that is, 1.25 dB worse than ideal PSK.

In general, the accuracy of bit error rate estimates using the error counting method may be characterized by the number of errors counted, n , and the probability of error, P_e . In the limit as n approaches infinity, the estimate of the P_e will converge to the true value of P_e . For finite n , the reliability of the estimate is related to the expected probability of error. This relation may be defined in terms of confidence intervals. A confidence interval is a range of probability of error in which, for a given P_e , the probability or confidence that the estimated P_e is within this range is known. For example, Table 3-1 lists the 90-percent confidence intervals as a function of the number of errors, $n = 10, 20, 30, 40, 50$, and 100. A complete discussion and derivation of confidence level estimation is given in [Ref. 3]. The simulation runs presented in this report were, for the most part, computed using $n \geq 100$. In the cases where probability of error estimates extended lower than $P_e = 1 \times 10^{-3}$, the number of errors counted for some of the measurements was in the range shown in Table 3-1.

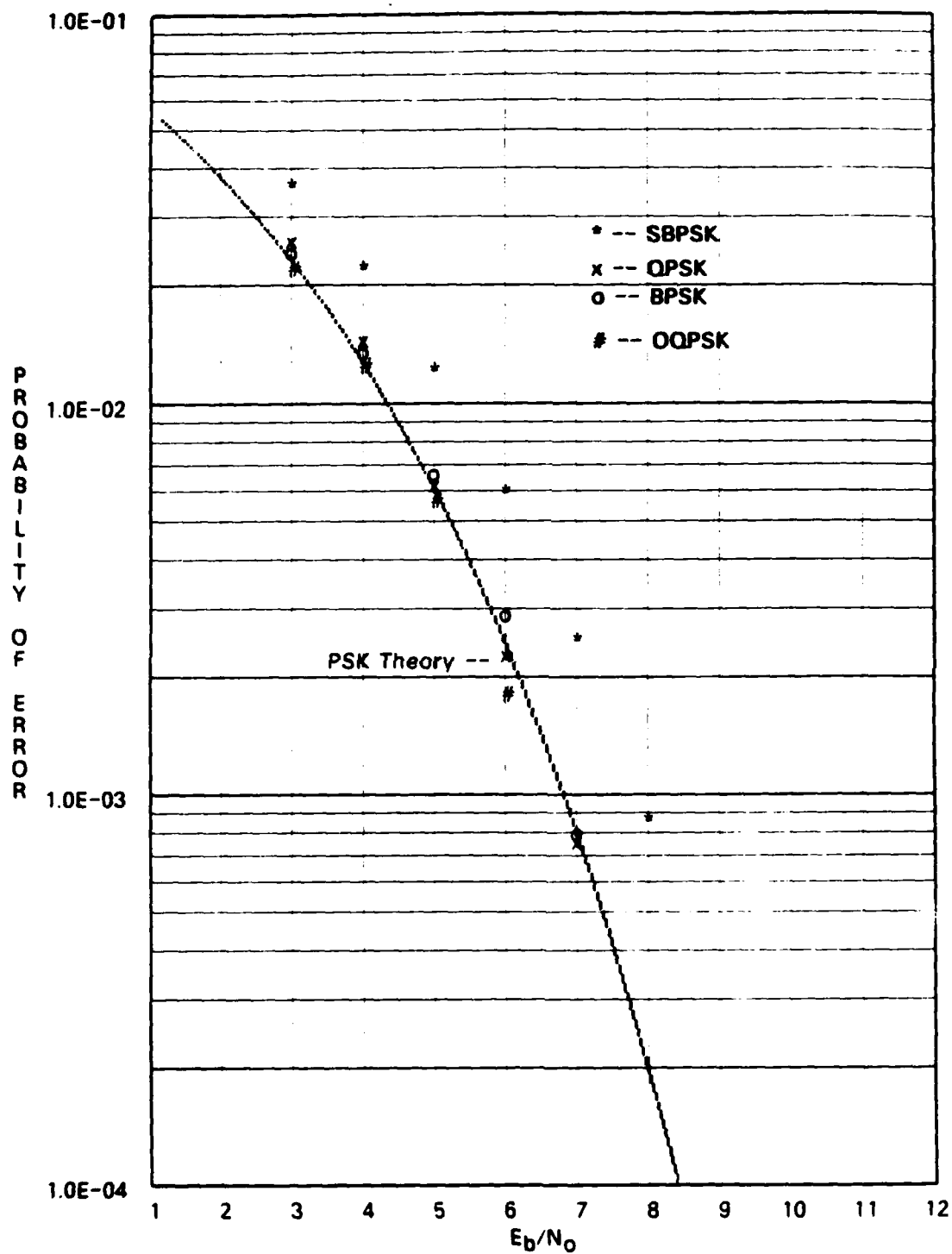


Figure 3-3. Verification of Simulator BER Estimates Theory of PSK with Gaussian Noise Interference

Table 3-1. Ninety Percent Confidence Intervals for n Errors and Probability of Error, p

n ERRORS	90% CONFIDENCE INTERVAL
10	$0.597 \times p$ TO $1.675 \times p$
20	$0.693 \times p$ TO $1.443 \times p$
30	$0.741 \times p$ TO $1.350 \times p$
40	$0.771 \times p$ TO $1.297 \times p$
50	$0.792 \times p$ TO $1.262 \times p$
100	$0.848 \times p$ TO $1.179 \times p$

803148.0

CHAPTER 4

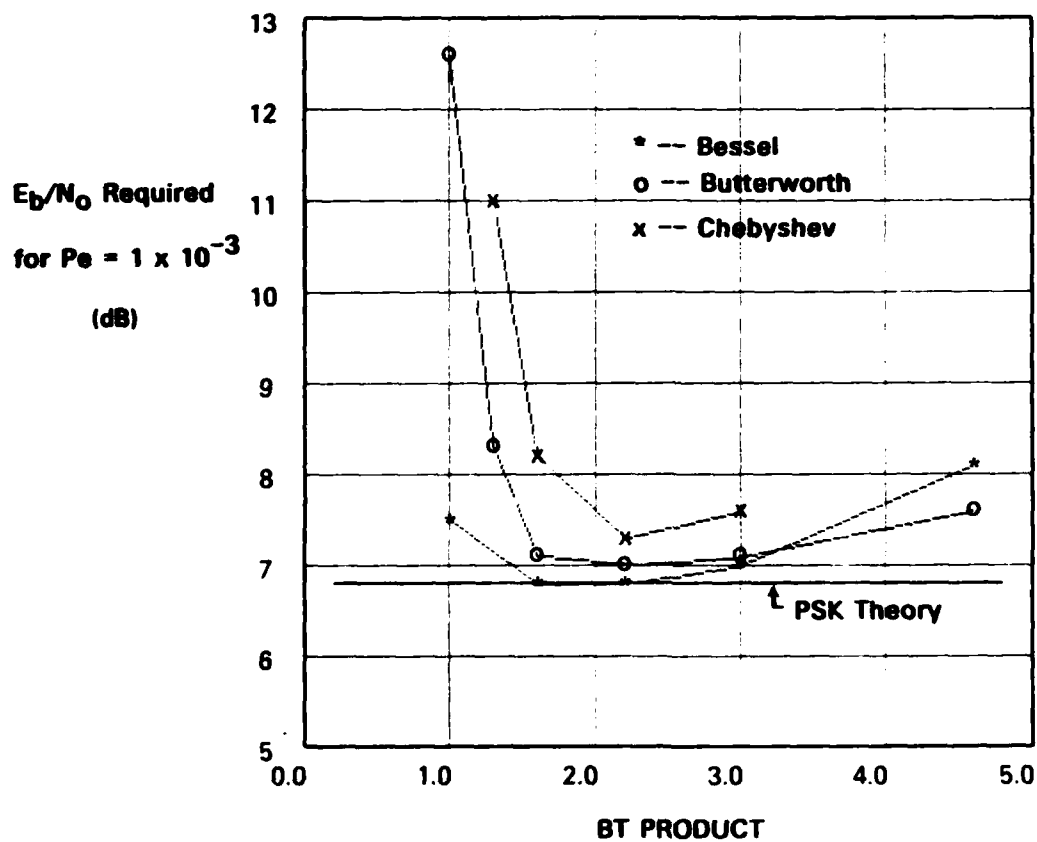
RESULTS

4.1 REQUIRED E_b/N_0 FOR GIVEN P_e vs. FILTER BT

This section presents the results of the simulation runs in terms of the E_b/N_0 required for a given P_e . Results are presented for the Bessel, Butterworth, and Chebyshev filters over a wide range of filter BT products. The modulation, bit rate and channel spacings used in the runs are associated with current and planned MILSATCOM systems. For BPSK and SBPSK 5-kHz channels, the results were derived for $P_e = 1 \times 10^{-3}$ -- the worst-case value acceptable for voice reception. For QPSK and OQPSK the results were derived a channel error rate of $P_e = 5 \times 10^{-2}$. This is the channel error rate corresponding to a decoded error rate of $P_e = 1 \times 10^{-5}$ for $K=7$, $R=1/2$, convolutional coding with soft decision (3-bit) decoding assuming the interference has the properties of Gaussian noise [Ref. 4]. In this and following chapters the term S_{iu}/S_d is used to define the ratio of the upper frequency interfering adjacent channel signal power to desired (central) channel signal power in dB; similarly, S_{il}/S_d is the ratio of lower frequency interfering adjacent channel signal power to desired (central) channel signal power ratio in dB.

4.1.1 BPSK - 5-kHz Channels

Figure 4-1 depicts the E_b/N_0 required for $P_e = 1 \times 10^{-3}$ versus filter BT product for the Bessel, Butterworth and Chebyshev filters. The channel symbol rate (R_s) is 2400 sps and the channel includes balanced uplink and downlink noise levels and equal power adjacent channel interferers ($S_{iu}/S_d = S_{il}/S_d = 0$ dB) spaced at 10 kHz from the middle of the center channel.



603185.0

Figure 4-1. Performance of BPSK for Selected 8-Pole Filters. Channel Characteristics: $R_b = 1/T = 2400$ sps; Equal Power Interferers at ± 10 kHz; Balanced Uplink and Downlink Noise Levels; 5-kHz Channels

Figure 4-1 illustrates that in the region of $BT < 2$, the required E_b/N_0 is significantly increased due to ISI caused by heavy filtering. In the region of $BT > 3$, the required E_b/N_0 is increased due to ACI because of insufficient out-of-band filtering. The Bessel filter performs slightly better than the Chebyshev and Butterworth filters, although, there is less than a 0.5-dB difference in the E_b/N_0 required for the three filter types in the region $2 < BT < 3$. Performance with the Bessel filter is also the least sensitive to changes in the BT product. This is because the Bessel filter has the widest transition band of the three filter types and causes the least amount of phase distortion.

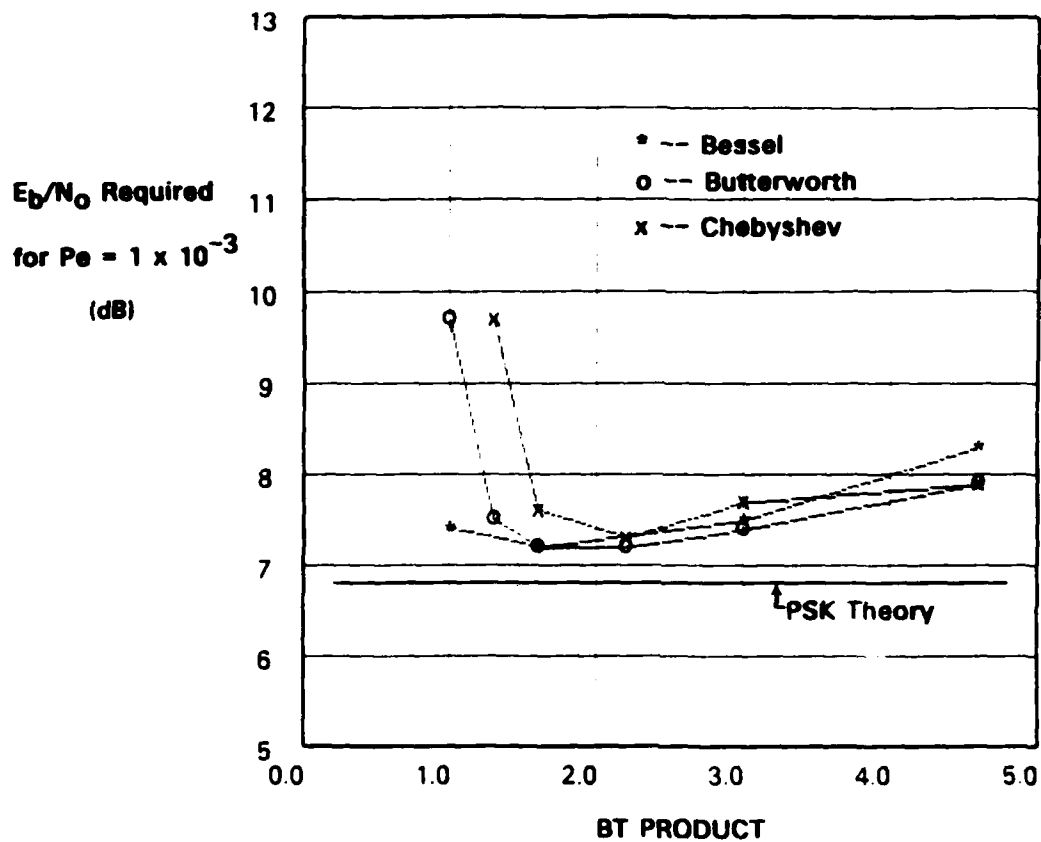
4.1.2 SBPSK - 5-kHz Channels

Figure 4-2 depicts the E_b/N_0 required for SBPSK with $P_e = 1 \times 10^{-3}$ versus filter BT product for the Bessel, Butterworth, and Chebyshev filters. The channel symbol rate (R_s) is 2400 sps, and the channel includes balanced uplink and downlink noise levels and equal power adjacent channel interferers ($S_{iu}/S_d = S_{il}/S_d = 0$ dB) spaced at 10 kHz from the central channel frequency.

Results in Figure 4-2 for SBPSK exhibit the same performance trends as those observed in Figure 4-1 for BPSK. A comparison of the figures shows that SBPSK requires slightly higher E_b/N_0 (up to 0.5 dB) than BPSK. As discussed earlier, this is due to the non-ideal implementation used to model SBPSK to be consistent with practical SBPSK receiver implementations in the field.

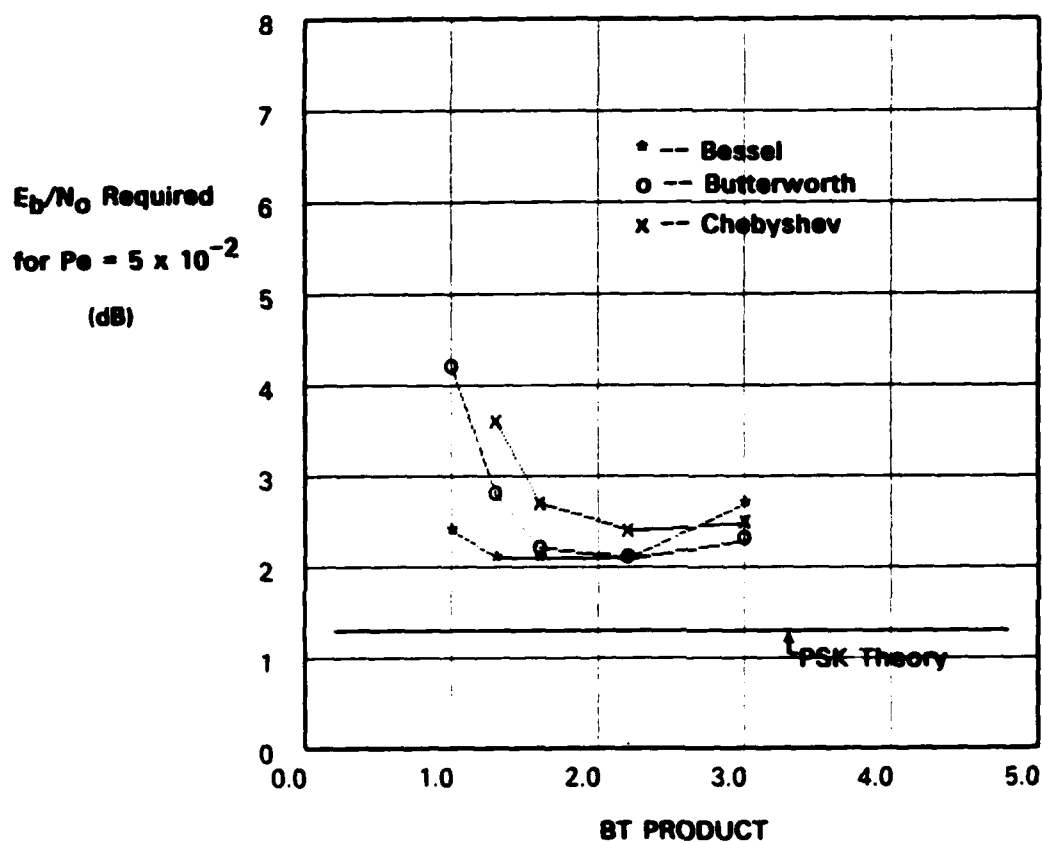
4.1.3 QPSK - 25-kHz Channels

Figure 4-3 depicts the E_b/N_0 required for $P_e = 5 \times 10^{-2}$ versus filter BT product for the Bessel, Butterworth, and Chebyshev filters. The channel symbol rate (R_s) is 16000



603189.0

Figure 4-2. Performance of SBPSK for Selected 8-Pole Filters. Channel Characteristics: $R_s = 1/T = 2400$ sps; Equal Power Interferers at ± 10 kHz; Balanced Uplink and Downlink Noise Levels; 5-kHz Channels



803188.0

Figure 4-3. Performance of QPSK for Selected 8-Pole Filters. Channel Characteristics: $R_b = 1/T = 16000$ sps; Equal Power Interferers at ± 50 kHz; Balanced Uplink and Downlink Noise Levels; 25-kHz Channels

sps, and the channel includes balanced uplink and downlink noise levels and equal power adjacent channel interferers ($S_{iu}/S_d = S_{il}/S_d = 0$ dB) spaced at ± 50 kHz from the central channel frequency.

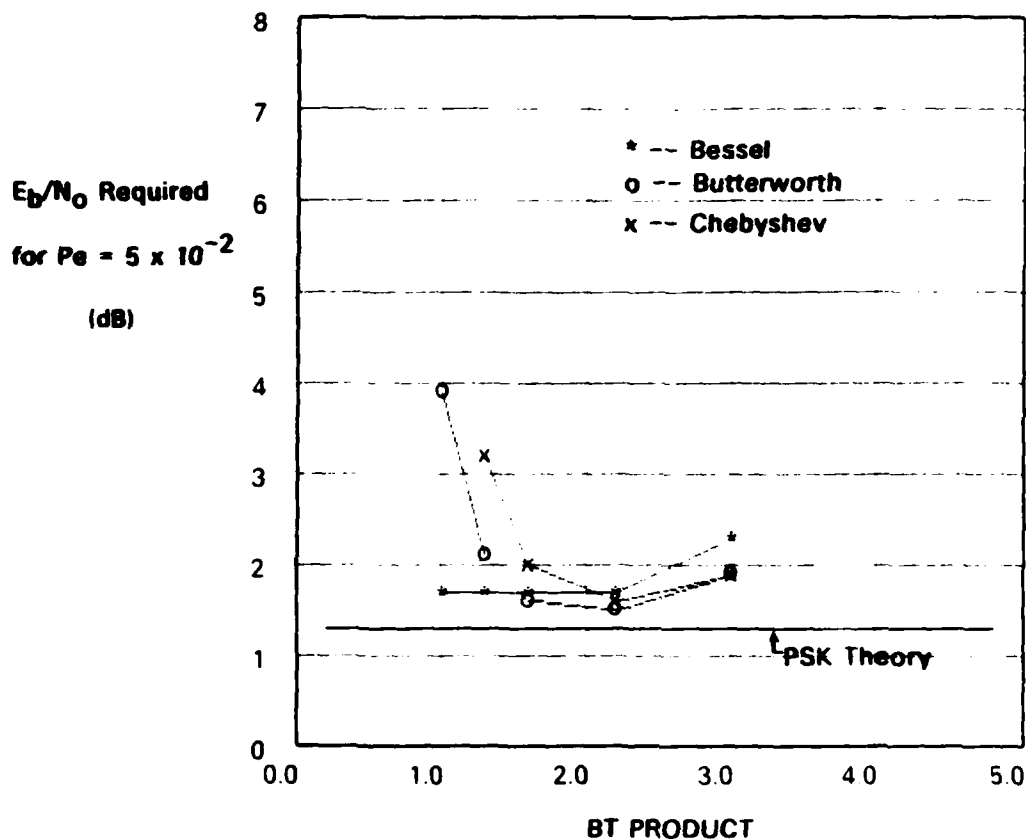
4.1.4 OQPSK - 25-kHz Channels

Figure 4-4 depicts the E_b/N_0 required for $P_e = 5 \times 10^{-2}$ versus filter BT product for the Bessel, Butterworth, and Chebyshev filters. The channel symbol rate (R_s) is 16000 sps, and the channel includes balanced uplink and downlink noise levels and equal power adjacent channel interferers ($S_{iu}/S_d = S_{il}/S_d = 0$ dB) spaced at 50 kHz from the central channel frequency.

A comparison of Figures 4-3 and 4-4 indicate that OQPSK offers approximately 1 dB better performance than QPSK for this particular channel. All of the filters offer approximately the same performance in the range $2 < BT < 3$. The Bessel filter requires slightly higher E_b/N_0 in this range. This is because the transition band is wider than the other filters and therefore a higher level of ACI enters the desired channel. However, with equal-power interferers and small BT values (e.g. $BT < 1.5$), the Bessel filter provides better performance than that of the Butterworth and Chebyshev filters.

4.2 REQUIRED E_b/N_0 FOR GIVEN P_e VS FILTER BT WITH INCREASED POWER INTERFERERS

This section investigates the performance of BPSK and SBPSK 5- and 25-kHz channels when subjected to high levels of adjacent channel interference power. As in the previous section the results are presented in terms of the E_b/N_0 required for a given P_e . The channel spacings and adjacent channel signal power levels investigated in this section were chosen to characterize the channel performance under the most stringent conditions which are likely to exist in practical use.



603196.0

Figure 4-4. Performance of OQPSK for Selected 8-Pole Filters. Channel Characteristics: $R_s = 1/T = 16000$ sps; Equal Power Interferers at ± 50 kHz; Balanced Uplink and Downlink Noise Levels; 25-kHz Channels

The 5-kHz channel results are obtained with adjacent channel interferers at 5-kHz and 10-kHz spacing. The adjacent channel signal power to desired (central) channel signal power ratio is +3 dB for 5-kHz spacing and +10 dB for 10-kHz spacing (i.e., $S_{il}/S_d = S_{iu}/S_d = 3$ dB for 5-kHz spacing and $S_{il}/S_d = S_{iu}/S_d = 10$ dB for 10-kHz spacing).

The 25-kHz channel results are obtained with adjacent channel interferers at 50-kHz and 100-kHz spacing. The adjacent channel signal power to desired (central) channel signal power ratio is +10 dB for these channels (i.e., $S_{il}/S_d = S_{iu}/S_d = 10$ dB).

4.2.1 BPSK - 5-kHz Channels

Figures 4-5 and 4-6 depict the E_b/N_0 required for $P_e = 1 \times 10^{-3}$ versus filter BT product for the Bessel, Butterworth and Chebyshev filters. The channel symbol rate (R_s) is 1200 sps and the channel includes balanced uplink and downlink noise levels. Figure 4-5 depicts the results for the channel with +3 dB power adjacent channel interferers ($S_{iu}/S_d = S_{il}/S_d = 3$ dB) spaced at 5 kHz from the middle of the center channel. Figure 4-6 depicts the results for the same channel with +10 dB power adjacent channel interferers ($S_{iu}/S_d = S_{il}/S_d = 10$ dB) spaced at 10 kHz from the center channel.

Figures 4-5 and 4-6 exhibit the same performance trends as those observed for the 10 kHz channel with equal power interferers (see Figure 4-1, Section 4.1.1). That is, the Bessel filter provides the best performance for $BT < 1.5$ and all three filter types provide comparable performance for BT products in the range 1.6 - 2.2. Figures 4-5 and 4-6 indicate that the Chebyshev filter requires a 1 dB higher E_b/N_0 than the Bessel and Butterworth for filter $BT = 3.0$. It is possible that the expected higher ACI rejection characteristic of the

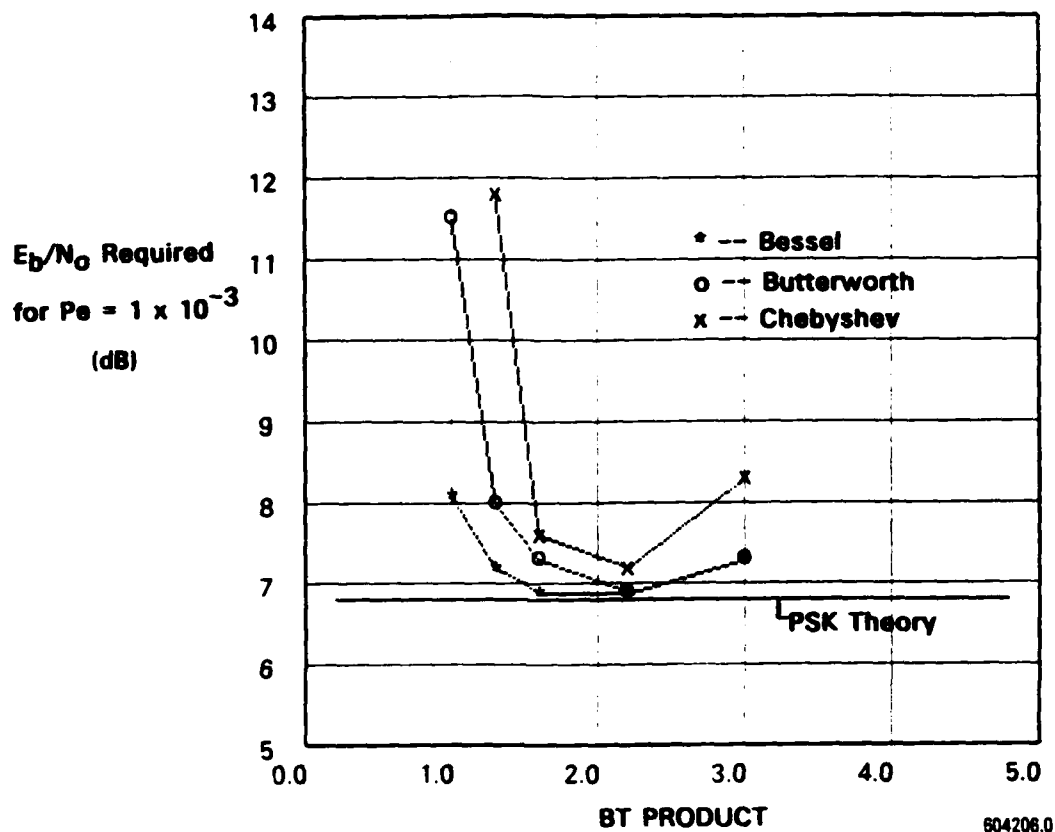


Figure 4-5. Performance of BPSK for Selected 8-Pole Filters. Channel Characteristics: $R_s = 1/T = 1200$ sps; +3 dB Power Interferers at ± 5 kHz; Balanced Uplink and Downlink Noise Levels; 5-kHz Channels

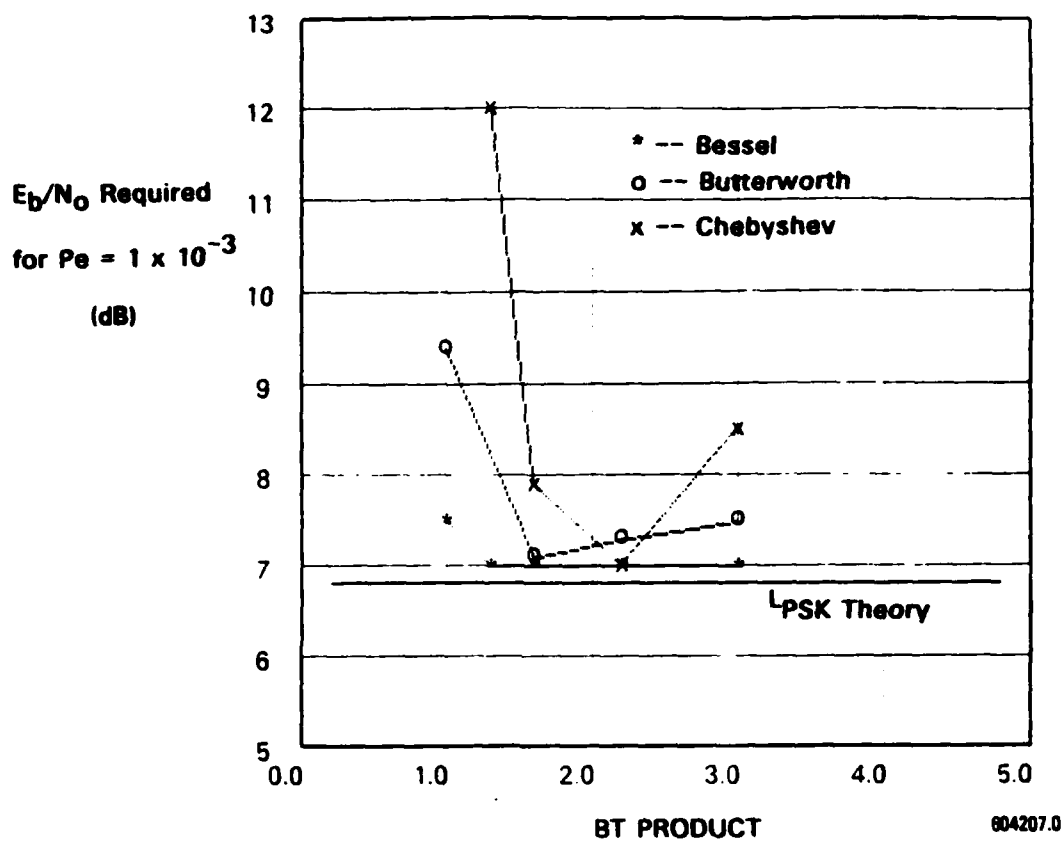


Figure 4-6. Performance of BPSK for Selected 8-Pole Filters. Channel Characteristics: $R_b = 1/T = 1200$ sps; + 10 dB Power Interferers at ± 10 kHz; Balanced Uplink and Downlink Noise Levels; 5-kHz Channels

Chebyshev filter is not realized for filter $BT < 4.0$ as seen in Figure 4-2. Further investigation would be required to determine the cause of this slight anomaly.

4.2.2 SBPSK - 5-kHz Channels

Figures 4-7 and 4-8 depict the E_b/N_0 required for $P_e = 1 \times 10^{-3}$ versus filter BT product for the Bessel, Butterworth and Chebyshev filters. The channel symbol rate (R_s) is 2400 sps and the channel includes balanced uplink and downlink noise levels. Figure 4-7 depicts the results for the channel with +3 dB power adjacent channel interferers ($S_{iu}/S_d = S_{il}/S_d = 3$ dB) spaced at 5 kHz from the middle of the center channel. Figure 4-8 depicts the results for the same channel with +10 dB power adjacent channel interferers ($S_{iu}/S_d = S_{il}/S_d = 10$ dB) spaced at 10 kHz from the center channel.

A comparison of Figures 4-7 and 4-8 demonstrates the performance trends of the SBPSK waveform in closely spaced channels. In Figure 4-7 where the nominal channel size is 5 kHz and the channel spacing is only 5 kHz, there is a high level of ACI due to the fact that the relatively broad main lobe of adjacent channels overlap. In Figure 4-8 where the channel spacing is increased to 10 kHz, the channel filters reject most of the interference from the adjacent channel's main lobe, and fast rolloff of the filtered sidelobes results in less degradation due to ACI. It is also apparent that because of the relatively high level of ACI in Figure 4-7 as compared to Figure 4-8, the E_b/N_0 required is more sensitive to the filter BT product in Figure 4-7.

4.2.3 BPSK - 25-kHz Channels

Figure 4-9 depicts the E_b/N_0 required for $P_e = 5 \times 10^{-2}$ versus filter BT product for the Bessel, Butterworth

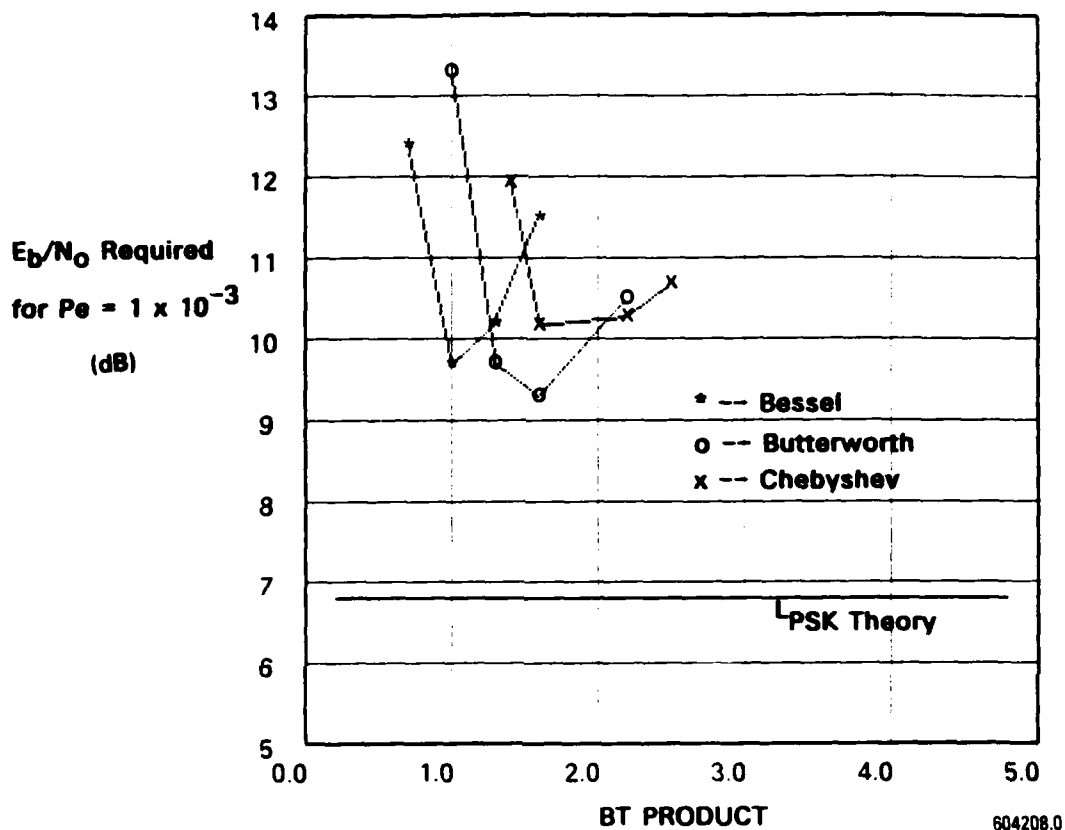


Figure 4-7. Performance of SBPSK for Selected 8-Pole Filters. Channel Characteristics: $R_s = 1/T = 2400$ sps; + 3 dB Power Interferers at ± 5 kHz; Balanced Uplink and Downlink Noise Levels; 5-kHz Channels

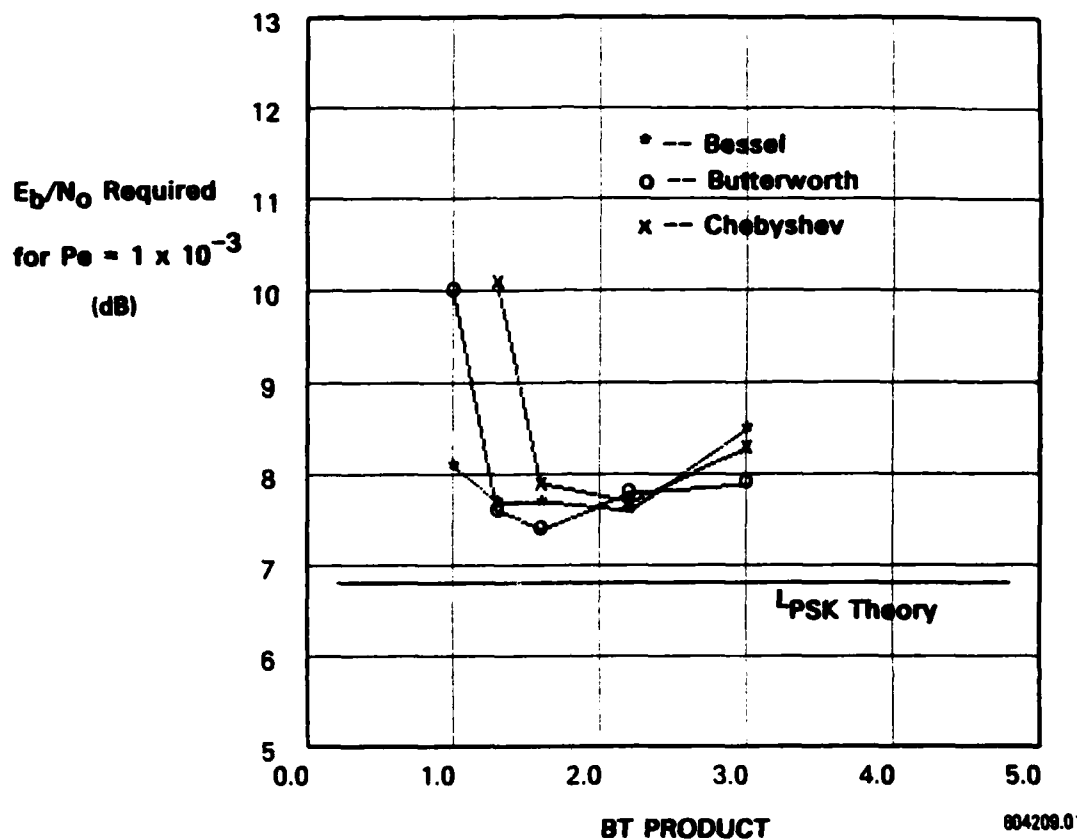


Figure 4-8. Performance of SBPSK for Selected 8-Pole Filters. Channel Characteristics: $R_s = 1/T = 2400$ sps; + 10 dB Power Interferers at ± 10 kHz; Balanced Uplink and Downlink Noise Levels; 5-kHz Channels

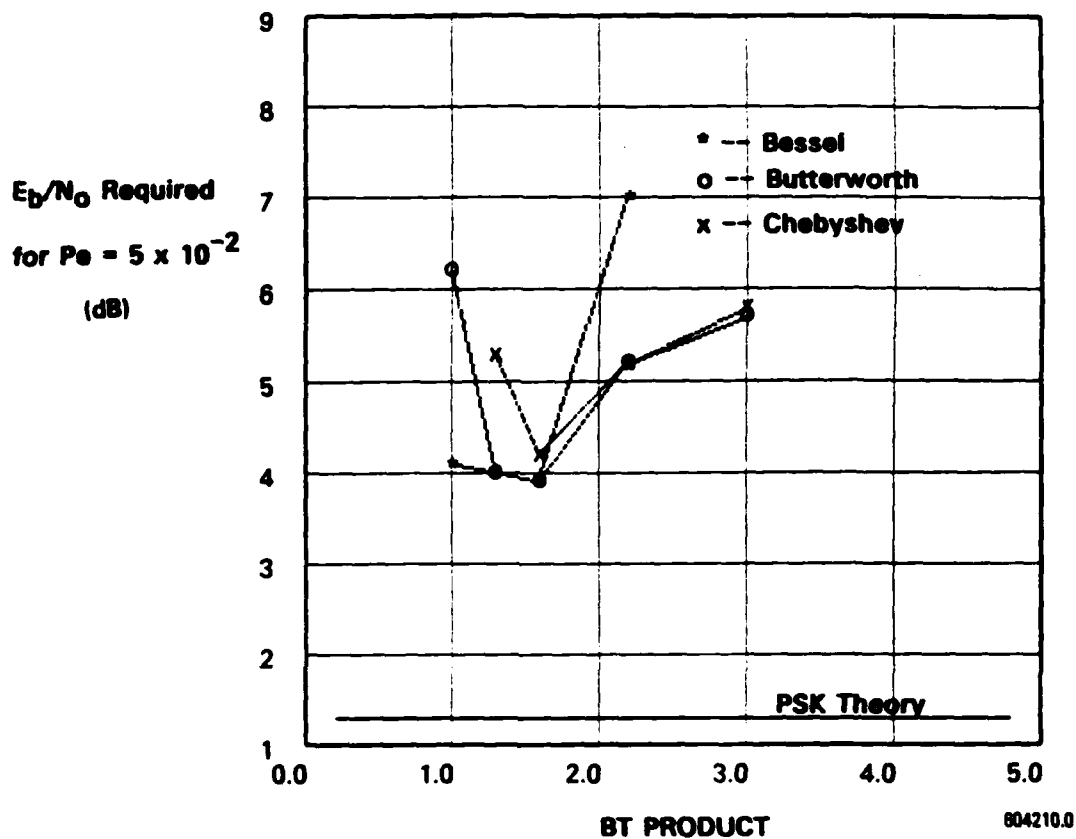


Figure 4-9. Performance of BPSK for Selected 8-Pole Filters. Channel Characteristics: $R_b = 1/T = 19.2$ kbps; + 10 dB Power Interferers at ± 50 kHz; Balanced Uplink and Downlink Noise Levels; 25-kHz Channels

and Chebyshev filters. The channel symbol rate (R_s) is 19.2 kbps and the channel includes balanced uplink and downlink noise levels and +10 dB power adjacent channel interferers ($S_{iu}/S_d = S_{il}/S_d = 10$ dB) spaced at 50 kHz from the middle of the center channel. Figure 4-10 depicts the results for the same channel with interferers spaced at 100 kHz from the middle of the center channel.

Figures 4-9 and 4-10 exhibit the same performance trends as the BPSK 10-kHz channels with respect to the effect of filter BT product on required E_b/N_0 . In Figure 4-9 performance is degraded by approximately 2.5 to 3.0 dB from theory for the three filters with BT products in the range $1.4 < BT < 1.6$. This degradation is due to the high level of ACI that cannot be rejected by the channel filters because of the close channel spacing and increased power of the interferers. In Figure 4-10 the performance is degraded by only approximately 1 dB in this range because the increased channel spacing reduces the level of in-band ACI.

4.2.4 SBPSK - 25-kHz Channels

Figure 4-11 depicts the E_b/N_0 required for $P_e = 5 \times 10^{-2}$ versus filter BT product for the Bessel, Butterworth and Chebyshev filters. The channel symbol rate (R_s) is 19.2 kbps and the channel includes balanced uplink and downlink noise levels and +10 dB power adjacent channel interferers ($S_{iu}/S_d = S_{il}/S_d = 10$ dB) spaced at 50 kHz from the middle of the center channel. Figure 4-12 depicts the results for the same channel with interferers spaced at 100 kHz from the middle of the center channel.

Figures 4-11 and 4-12 exhibit the same performance trends observed for the BPSK 25-kHz channels in Figures 4-9 and 4-10. However, a comparison of the figures also shows that total degradation for SBPSK is approximately 1.5 dB less than that

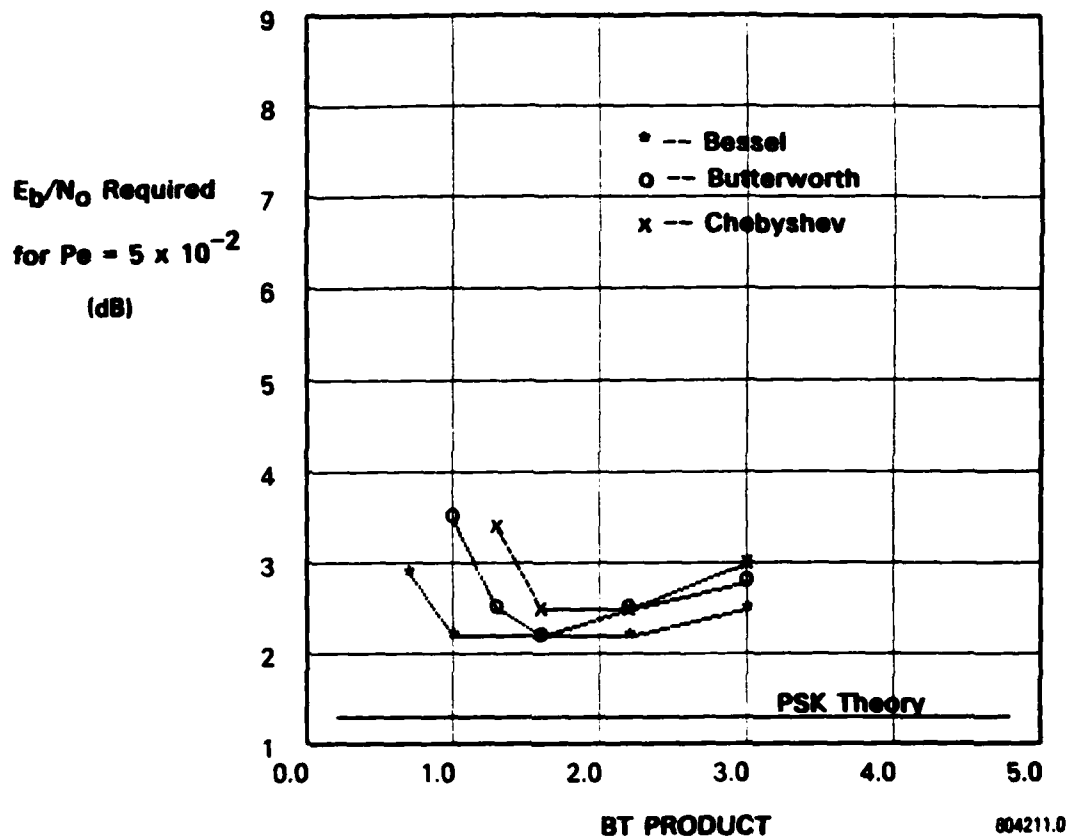


Figure 4-10. Performance of BPSK for Selected 8-Pole Filters. Channel Characteristics: $R_b = 1/T = 19.2$ kbps; + 10 dB Power Interferers at ± 100 kHz; Balanced Uplink and Downlink Noise Levels; 25-kHz Channels

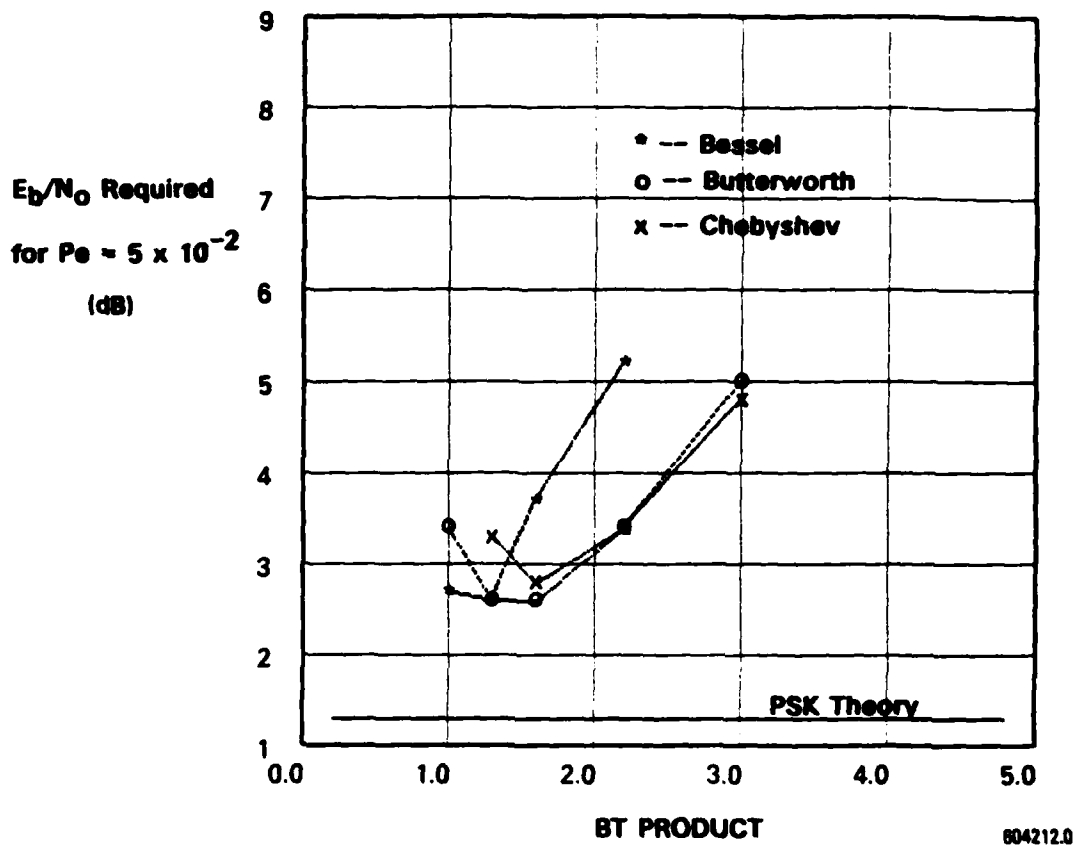
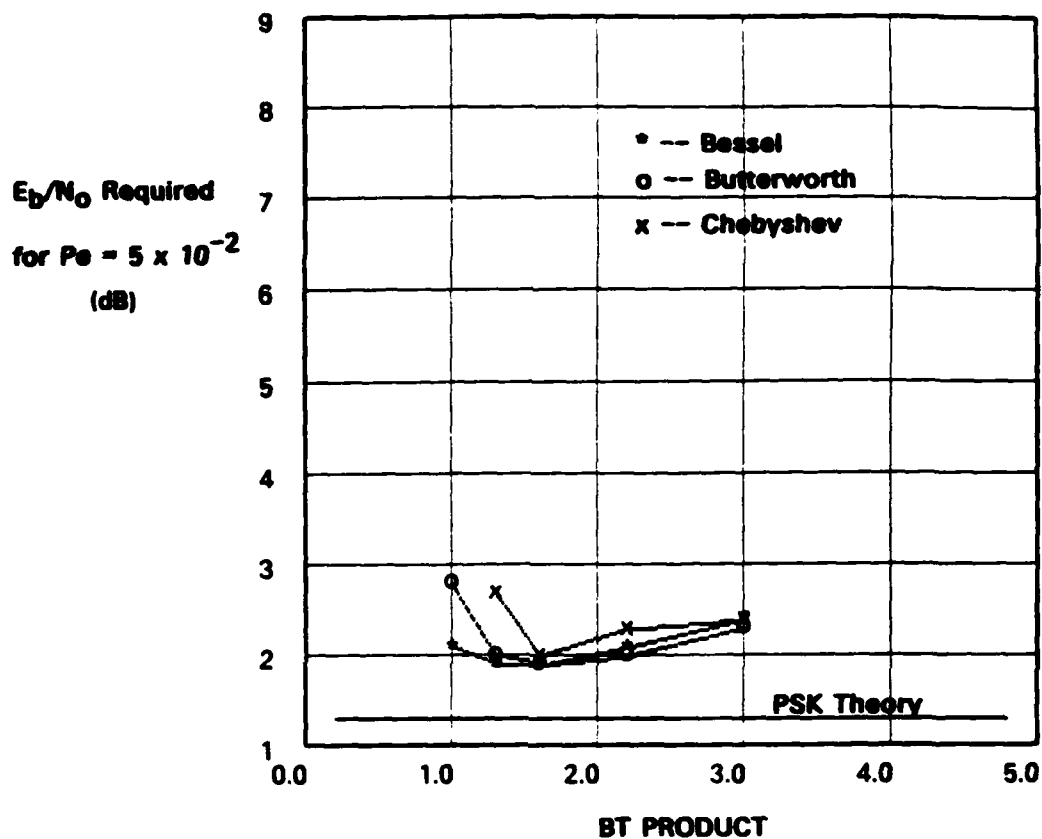


Figure 4-11. Performance of SBPSK for Selected 8-Pole Filters. Channel Characteristics: $R_b = 1/T = 19.2$ kps; +10 dB Power Interferers at ± 50 kHz; Balanced Uplink and Downlink Noise Levels; 25-kHz Channels



804213.0

Figure 4-12. Performance of SBPSK for Selected 8-Pole Filters. Channel Characteristics: $R_b = 1/T = 19.2$ kps; + 10 dB Power Interferers at ± 100 kHz; Balanced Uplink and Downlink Noise Levels ; 25-kHz Channels

for BPSK in the case of 50-kHz channel spacing. For 100-kHz channel spacing, because of the much lower level of ACI SBPSK and BPSK afford comparable performance.

CHAPTER 5

SUMMARY AND CONCLUSIONS

5.1 SUMMARY

This report provides the results of the MILSATCOM UHF nonlinear channel analysis. The study shows the effects on channel performance versus selected channel parameter values using a computer simulation of the channel. The simulation, through the addition of newly developed software modules, extends the scope of a previously developed channel model [Ref. 1] and provides estimates of channel performance in terms of P_e vs. E_b/N_o .

The results may be summarized for the 25-kHz and 5-kHz channel bandwidths as follows:

25-kHz Channels:

1. For narrow channels (filter $BT < 1.5$) with equal power interferers ($S_{iu}/S_{il}/S_d = 0$ dB, Figures 4-3 and 4-4), better performance (i.e., lower E_b/N_o required for a given BER) is afforded by using Bessel filters versus Chebyshev or Butterworth filters. This is because the Bessel filter's low phase distortion property has a greater influence on system performance than out-of-band power rejection at these relatively low levels of ACI.

2. For relatively wide channels (filter $BT > 2.5$), there appears to be little or no difference in performance provided by any of the three filter types (for $S_{iu}/S_d = S_{il}/S_d = 0$ dB, Figures 4-3 and 4-4).

3. For $S_{iu}/S_{id} = S_{il}/S_{id} = +10$ dB, ACI had a much greater influence on performance than observed for the equal ($S_{iu}/S_d = S_{il}/S_d = 0$ dB) case, particularly for the configurations having small channel spacing. Specifically,

a. For 50-kHz channel spacing, SBPSK outperforms BPSK consistently by an approximate 1.5-dB margin (Figures 4-9 and 4-11). Bessel filters afford the highest performance for filter $BT < 1.2$. All three filters provide comparable performance for filter BT s in the range of 1.5 to 1.6. For filter $BT > 2.5$, the high level of ACI substantially degrades system performance especially when the Bessel filter is used.

b. For 100-kHz channel spacing (Figures 4-10 and 4-12), because of the much lower level of ACI, SBPSK and BPSK afford comparable performance for filter $BT > 1.5$. BPSK suffers more degradation (approximately 1 dB) than SBPSK from ISI at smaller filter BT values when a Butterworth or Chebyshev filter is used.

5-kHz Channels:

1. For $S_{iu}/S_{id} = S_{il}/S_{id} = 0$ dB and 10-kHz channel spacing (Figures 4-1 and 4-2), similar results to those found with the 25-kHz channels were found. That is, for narrow channels with filter $BT < 1.5$, the Bessel filter provides superior performance over that provided by the Butterworth and Chebyshev filters and for relatively wide channels (filter $BT > 2.5$) little difference in performance is noted among the three filter types. As before, these results are expected because the relatively low level of ACI in the central channel has much less impact on performance than the ISI levels caused by the Butterworth and Chebyshev filters with small BT .

2. For $S_{iu}/S_{id} = S_{il}/S_{id} = +3$ dB two separate configurations were simulated:

a. BPSK at 1200 sps with channel spacing of 5 kHz (Figure 4-5) resulted in similar trends as before with some exceptions. Again, with narrow channel bandwidth, ISI was greatest (and performance worst) with Butterworth and Chebyshev filters. However, at filter $BT > 2.5$, the Chebyshev filter degraded system performance by about 1 dB greater than the Butterworth and Bessel filters. This apparent anomaly is noticeable only for BPSK at the 1200 sps symbol rate (see item 3. below). It is possible that the benefits afforded by a Chebyshev filter in rejecting ACI are not fully realized for filter $BT < 3.5 - 4.0$. Further investigation would be required to resolve this issue completely.

b. SBPSK at 2400 sps with channel spacing of 5 kHz (Figure 4-7) resulted in predictable trends with ISI causing degraded performance at small filter BT values and ACI degrading performance for large filter BT values. The Bessel filter minimized ISI and rejected the least ACI for a given filter BT ; the Chebyshev had just the opposite effects and the Butterworth performance was in between these two. Because of the narrow channel spacing and increased adjacent channel power levels, the system performance was very sensitive to a given filter's BT product.

3. For $S_{iu}/S_{id} = S_{il}/S_{id} = +10$ dB, two separate configurations were simulated:

a. SBPSK at 2400 sps with channel spacing of 10 kHz (Figure 4-8) has an approximate 0.5-dB performance degradation over that found for the case of $S_{iu}/S_{id} = S_{il}/S_{id} = 0$ dB. As in the latter configuration, little difference in performance is achieved by the different filter types for

BT > 1.5; for filter BT < 1.5 the Bessel filter affords the best performance, followed by the Butterworth and Chebyshev.

b. BPSK at 1200 sps with channel spacing of 10 kHz (Figure 4-6) and $S_{iu}/S_{id} = 10$ dB gives similar performance to the same channel configuration with $S_{iu}/S_{id} = S_{il}/S_{id} = +3$ dB. This result is likely due to the relatively wide channel spacing for this data rate and consequently ACI having a comparable effect on overall performance.

Tables 5-1 and 5-2 summarize the findings of this study and present recommended channel configurations (filter type and BT product) for modulation type, symbol rate, and channel spacing.

A previous study [Ref. 6] addressed channel spacing considerations by approximating the effects of ACI power as additive white gaussian noise. Appendix B, using consistent assumptions, compares the E_b/N_0 performance degradation based on the additive noise approximation with the results for the "best" filter in the present study. The results were consistent for BPSK. However, for SBPSK, the additive noise model was conservative, partially due to the false assumption that hardlimiting caused complete spectral tail regeneration.

5.2 CONCLUSIONS

This study has investigated MILSATCOM UHF parameter variations that were chosen to fully characterize the system under the most stringent conditions that are likely to exist in practical use. Filter specification and channel spacing tradeoffs were characterized in terms of ISI and ACI effects on bit error rate performance. In general, filters providing minimal phase distortion with BT products in the range of 1.8 to 2.2 were found to provide the highest performance. SBPSK

Table 5-1. Summary of Filter Performance for 5 kHz Channels at 1×10^{-3} Channel Error Rate

MODULATION TYPE	SYMBOL RATE	ADJACENT CHANNEL SPACING	ACI POWER ($S_u / S_d = S_u / S_d$)	FILTER TYPE *	E_b / N_0 AT OPTIMUM BT PRODUCT†
BPSK	2400 (bps)	10 (kHz)	0 (dB)	B	7.0 (dB)
				C	7.3
				S	6.8
BPSK	1200	5	3	B,S	6.9
				C	7.2
BSPK	1200	10	10	B,C,S	7.0
SBPSK	2400	10	0	B,S	7.2
				C	7.3
SBPSK	2400	5	3	B	9.3
				C	10.2
				S	9.7
SBPSK	2400	10	10	B	7.4
				C	7.7
				S	7.6

* B = BUTTERWORTH, C = CHEBYSHEV, S = BESSEL

† REQUIRED THEORETICAL $E_b/N_0 = 6.8$ dB

604229.0

Table 5-2. Summary of Filter Performance for 25 kHz Channels at 5×10^{-2} Channel Error Rate

MODULATION TYPE	SYMBOL RATE	ADJACENT CHANNEL SPACING	ACI POWER ($S_{in} / S_d = S_R / S_d$)	FILTER TYPE *	E_b / N_0 AT OPTIMUM BT PRODUCT†
BPSK	19200(bps)	50 (kHz)	10 (dB)	B,S C	3.9 (dB) 4.2
BPSK	19200	100	10	B,S C	2.2 2.5
SBPSK	19200	50	10	B,S C	2.6 2.8
SBPSK	19200	100	10	B,S C	1.9 2.0
QPSK	16000	50	0	B,S C	2.1 2.4
OQPSK	16000	50	0	B C S	1.5 1.6 1.7

* B = BUTTERWORTH, C = CHEBYSHEV, S = BESSEL

† REQUIRED THEORETICAL $E_b/N_0 = 1.3$ dB
WITH 3-BIT SOFT-DECISION VITERBI CODING

604231.0

and OQPSK were found to provide better E_b/N_0 performance than BPSK and QPSK only under conditions of high adjacent channel interferers with small channel spacings (e.g., 5 kHz for 5-kHz channels, and 50 kHz for 25-kHz channels).

5.3 RECOMMENDATIONS FOR FUTURE STUDY

Future studies in this area should focus on investigating effects of hybrid filters providing both good out-of-band rolloff and minimal phase distortion, such as an equalized Chebyshev filter, in conjunction with spectrally efficient modulation techniques, such as minimum shift-key (MSK). The combination of these system parameter characteristics will likely provide a near-optimal (in terms of performance and channel efficiency) configuration in future MILSATCOM UHF system design.

APPENDIX A
REFERENCES

1. Defense Communications Agency MILSATCOM Systems Office, Nonlinear Effects on PSK Spectra (U), November 1985 (Unclassified).
2. A.J. Viterbi, Principles of Coherent Communication. New York: McGraw Hill, 1966.
3. M.C. Jeruchim, "Techniques for Estimating the Bit Error Rate in the Simulation of Digital Communication Systems," IEEE Journal on Selected Areas of Communications, SAC-2, 1 (January 1984), 153-170.
4. HQ USAF ACS Studies and Analysis, Error Control Coding Handbook (U), July 1976 (Unclassified).
5. M. J. Dapper and T. J. Hill, "SBPSK: A Robust Bandwidth-Efficient Modulation for Hard-Limited Channels" (Unpublished). The authors are with Cincinnati Electronics, Cincinnati, Ohio.
6. Defense Communications Agency MILSATCOM Systems Office, Channel Spacing Considerations for Follow-on UHF MILSATCOM (U), November 1985 (Unclassified).

APPENDIX B

COMPARISON TO PREVIOUS RESULTS

A previous study [Ref. 6] addressed the channel spacing considerations by approximating the effects of cross-channel¹ interference power as additive white gaussian noise. The prior study also assumed that when filtered signals were hardlimited, the signal spectrum tails (sidebands) would be fully regenerated, causing interference on the downlink. Furthermore, the prior study did not consider the effects of inband filtering losses due to intersymbol interference. The purpose of this appendix is to compare the predicted degradation using this prior analytic model with that provided by the current simulation model.

The channel simulation used in the body of this report, addresses these questions and further addresses the questions on selection of filter type, poles, and bandwidths. The simulation model accurately models spectrum tail regrowth. The body of this report trades intersymbol interference off with adjacent channel interference through filter selection, resulting in the minimum net effect. This appendix compares the two models assuming the "best" filter was selected based on the simulation. Table B-1 addresses the capabilities of the modulation simulation model with the additive noise approximation model.

Assumptions are chosen to be consistent between the two models. The additive noise approximation model incorporates two adjacent channel interferers. An operating point is found

¹This study considered cross-channel interference from not only the two adjacent channels, but all nearby channels within a 500-kHz band.

Table B-1. Comparison of Modulation Simulation Model with Additive Noise Approximation Model

FEATURE	SIMULATION	ADDITIVE NOISE APPROXIMATION
EFFECTS CONSIDERED		
INTERSYMBOL INTERFERENCE	YES	NO
CROSS-CHANNEL INTERFERENCE		
ADJACENT	YES	YES
OTHER CHANNELS	NO	YES
POST LIMITER	YES	(APPROXIMATED BY FULL TAIL REGROWTH)
PHASE NONLINEARITIES	YES	NO
INTERMODULATION PRODUCTS	NO	YES (ADDRESSED IN GENERAL MANNER)
FILTER PARAMETERS		
TYPE FILTER	YES	NO
(I.e., BUTTERWORTH, BESSEL, & CHEBYSHEV)		DOUBLE "A" FILTER 3 BW _s
NUMBER OF POLES	6, 8	2
BANDWIDTH	A WIDE RANGE	ONLY 4, 5, 25 kHz
MODULATION	BPSK, QPSK, OQPSK, SBPSK	PSK, MSK, SBPSK (APPROXIMATED)
C/I VALUES	CAN BE GENERATED WITH FRACTIONAL OUT-OF-BAND POWER PROGRAM	YES
WHERE DEGRADATION MEASURED	THRESHOLD, UP & DOWN LINKS COMBINED	RANGE OF VALUES EACH LINK SEPARATE MUST BE COMBINED SEPARATELY

604201.0

such that the resultant C/kT is at the threshold for proper operation to be consistent with the assumptions used in the body of this report using the simulation model. Table B-2 compares the results of the additive noise approximation model with the simulation model. SBPSK was handled two ways. Based on simulations of SBPSK with 50-percent shaping resulting in a 1.2-decibel degradation, this amount was added to the required C/kT . Since this also increased the corresponding interferers by the corresponding ratio (interferers were 3 or 10 decibels larger than the desired signal), the resulting degradation became quite large. Alternatively, the 1.2 decibels were completely disregarded and the results were closer to those of the simulation.

Overall, the degradation predicted by the additive noise approximation was quite consistent with the simulation for BPSK. For SBPSK the additive noise model was somewhat conservative, partially due to the false assumption that hardlimiting caused complete spectrum tail regrowth.

Table B-2. Comparison of Degradations of Additive Noise Approximation to Modulation Simulation

NOMINAL CHANNEL BANDWIDTH (kHz)	SPACING (kHz)	MODULATION	RATE SYMBOLS PER SECOND	Δ POWER	C/KT UP & DOWN	C/KT IDEAL	CB/(KT β + I)	DEGRADATION	SIMULATION RESULT DEGRADATION
5	10	BPSK	2400	10	46.45	43.20	40.60	2.60	2.7
5	10	SBPSK	2400	10	45.55	42.24	41.80*	1.65*	.6
25	100	BPSK	19200	10	48.90	45.24	44.13	1.11	1.0
25	50	BPSK	19200	10	49.74	46.19	44.13	2.06	1.5
5	5	SBPSK	2400	3	49.00	45.86	41.81*	5.24*	2.5
5	5	BPSK	2400	3	47.31	44.10	40.60	3.50	—
5	5	BPSK	1200	3	42.19	38.57	37.59	.99	.1
5	10	BPSK	1200	10	42.02	38.38	37.59	.79	.2
5	10	SBPSK	2400	10	44.41	41.02	40.60	.42	.6
5	5	SBPSK	2400	3	46.76	43.53	40.60	2.93	2.5

* ALLOWS - 1.2 dB DEGRADATION FROM SBPSK DEMODULATION USING BPSK DEMODULATOR

UNCLASSIFIED

SECURITY CLASSIFICATION OF THIS PAGE

AD-A167733

REPORT DOCUMENTATION PAGE

Form Approved
OMB No. 0704-0188
Exp. Date: Jun 30, 1986

1a. REPORT SECURITY CLASSIFICATION UNCLASSIFIED		1b. RESTRICTIVE MARKINGS	
2a. SECURITY CLASSIFICATION AUTHORITY N/A		3. DISTRIBUTION/AVAILABILITY OF REPORT <i>Unlimited</i>	
2b. DECLASSIFICATION/DOWNGRADING SCHEDULE N/A		5. MONITORING ORGANIZATION REPORT NUMBER(S)	
4. PERFORMING ORGANIZATION REPORT NUMBER(S) Log No. MSO-86-037a		7a. NAME OF MONITORING ORGANIZATION Defense Communications Agency MILSATCOM Systems Office, Code A800	
6a. NAME OF PERFORMING ORGANIZATION M/A-COM LINKABIT, Inc.	6b. OFFICE SYMBOL (if applicable)	7b. ADDRESS (City, State, and ZIP Code) Washington, D.C. 20305-2000	
6c. ADDRESS (City, State, and ZIP Code) 8619 Westwood Center Drive Vienna, VA 22180		9. PROCUREMENT INSTRUMENT IDENTIFICATION NUMBER	
8a. NAME OF FUNDING/SPONSORING ORGANIZATION Defense Communications Agency	8b. OFFICE SYMBOL (if applicable) A800	10. SOURCE OF FUNDING NUMBERS	
8c. ADDRESS (City, State, and ZIP Code) 8th & S. Courthouse Road Arlington, VA 22204		PROGRAM ELEMENT NO.	PROJECT NO.
		TASK NO.	WORK UNIT ACCESSION NO.
11. TITLE (Include Security Classification) Channelization Considerations for PSK Modulation Techniques in Follow-on UHF MILSATCOM Systems (U)			
12. PERSONAL AUTHOR(S) Paul Chapell, Steven Hryckiewicz			
13a. TYPE OF REPORT Final Technical	13b. TIME COVERED FROM 4/1/86 TO 4/30/86	14. DATE OF REPORT (Year, Month, Day) 1986 April 30	15. PAGE COUNT 58
16. SUPPLEMENTARY NOTATION			
17. COSATI CODES		18. SUBJECT TERMS (Continue on reverse if necessary and identify by block number)	
FIELD	GROUP	SUB-GROUP	
19. ABSTRACT (Continue on reverse if necessary and identify by block number) (U) The purpose of this report is to develop channel spacing tradeoffs and requirements for the follow-on FLTSAT/LEASAT UHF MILSATCOM satellite system. It presents the results for MILSATCOM UHF 5-kHz and 25-kHz nonlinear (hardlimited) channel performance as a function of PSK modulation type and symbol rate, filter characteristics (type and bandwidth), and adjacent channel spacing. The primary channel performance measure is transmitted bit energy per channel noise (E_b/N_0) versus probability of bit error.			
20. DISTRIBUTION/AVAILABILITY OF ABSTRACT <input checked="" type="checkbox"/> UNCLASSIFIED/UNLIMITED <input type="checkbox"/> SAME AS RPT <input type="checkbox"/> DTIC USERS		21. ABSTRACT SECURITY CLASSIFICATION UNCLASSIFIED	
22a. NAME OF RESPONSIBLE INDIVIDUAL William Long		22b. TELEPHONE (Include Area Code) (703) 692-0280	22c. OFFICE SYMBOL A820

END

DTIC

6-86